THE JOURNAL OF BIOLOGICAL CHEMISTRY VOL. 285, NO. 38, pp. 29608–29622, September 17, 2010

A Conserved E7-derived Cytotoxic T Lymphocyte Epitope Expressed on Human *Papillomavirus* 16-transformed HLA-A2$^+$ Epithelial Cancers[S]

Received for publication, March 24, 2010, and in revised form, May 20, 2010 Published, JBC Papers in Press, July 8, 2010, DOI 10.1074/jbc.M110.126722

Angelika B. Riemer[‡§1,2], Derin B. Keskin[§1], Guanglan Zhang[‡], Maris Handley[‡§], Karen S. Anderson[‡], Vladimir Brusic[‡], Bruce Reinhold[‡§], and Ellis L. Reinherz[‡§3]

From the [‡]Cancer Vaccine Center and [§]Laboratory of Immunobiology, Department of Medical Oncology, Dana-Farber Cancer Institute, Harvard Medical School, Boston, Massachusetts 02115

Human *Papillomavirus* 16 (HPV-16) has been identified as the causative agent of 50% of cervical cancers and many other HPV-associated tumors. The transforming potential/tumor maintenance capacity of this high risk HPV is mediated by two viral oncoproteins, E6 and E7, making them attractive targets for therapeutic vaccines. Of 21 E6 and E7 peptides computed to bind HLA-A*0201, 10 were confirmed through TAP-deficient T2 cell HLA stabilization assay. Those scoring positive were investigated to ascertain which were naturally processed and presented by surface HLA molecules for CTL recognition. Because IFNγ ELISpot frequencies from healthy HPV-exposed blood donors against HLA-A*0201-binding peptides were unable to identify specificities for tumor targeting, their physical presence among peptides eluted from HPV-16-transformed epithelial tumor HLA-A*0201 immunoprecipitates was analyzed by MS^3 Poisson detection mass spectrometry. Only one epitope ($E7_{11-19}$) highly conserved among HPV-16 strains was detected. This 9-mer serves to direct cytolysis by T cell lines, whereas a related 10-mer ($E7_{11-20}$), previously used as a vaccine candidate, was neither detected by MS^3 on HPV-transformed tumor cells nor effectively recognized by 9-mer specific CTL. These data underscore the importance of precisely defining CTL epitopes on tumor cells and offer a paradigm for T cell-based vaccine design.

The transforming potential of human *Papillomavirus* (HPV),[4] first suspected in the 1970s, has now been firmly established both biologically and epidemiologically (1–3). The single most important variable linked to malignant transformation is persistent infection with one of the high-risk HPV types. The E6 and E7 proteins encoded by high-risk HPVs have transforming activities and functionally inactivate the p53 and retinoblastoma (Rb) tumor suppressor proteins, respectively (3, 4). HPV-16 is the most abundant high risk HPV and has been detected in >50% of cervical cancer cases and in most other HPV-induced tumors, such as carcinomas of the vagina, anus, vulva, penis, and oropharynx (3, 5, 6). Worldwide, high risk HPVs are thought to be responsible for >500,000 malignancies per year, representing more than 5% of human cancers (7).

A major breakthrough in combating HPV-induced disease was the development of prophylactic vaccines to prevent HPV infection in previously unexposed individuals. These vaccines are based on virus-like particles consisting of the L1 capsid protein (8, 9). Virus-like particles resemble natural virions and are able to induce high titers of L1-neutralizing antibodies. Two vaccines, one against HPV-16, -18, -6, and -11 and another against HPV-16 and -18, were approved for clinical use in 2006 (10–12). Although the impact of prophylactic HPV vaccination on the incidence of vaccine type HPV-associated disease and cancer is unquestionable over time, these vaccines have no therapeutic efficacy for established HPV infections. Antibodies neutralize virus particles only before infection. Moreover, as HPV capsid proteins are exclusively expressed late in the viral replication cycle within the upper layers of the epithelium, immune responses against capsid proteins do not affect persistently infected basal cells and, thus, fail to clear the infection (13). Moreover, high risk HPV-associated cancers generally represent nonproductive infections, and the capsid proteins are not expressed (5, 6). For these reasons, viral capsid based strategies are not useful in the development of therapeutic HPV vaccines.

HPV-16 infection is widespread in the sexually active population, but >95% of infections are either transient and/or cleared by the immune system (13). Regression of lesions has been shown to be dependent on strong localized cell-mediated immune responses. In particular, antigen-specific T cell-mediated immunity is required for the clearance of persistent high-risk HPV infections (14). Hence, the immune system is capable of terminating high risk HPV-associated lesions and tumors. Therapeutic vaccines aimed to induce targeted T cell-mediated immune responses against dysplastic and neoplastic cells, therefore, seem a logical extension for achieving beneficial clinical results. Given that E6 and E7 are consistently expressed in HPV-associated cancers, these proteins themselves represent promising targets for vaccine design. Although most tumor-

[S] The on-line version of this article (available at http://www.jbc.org) contains supplemental S1–S4.

[1] Both authors contributed equally to this work.

[2] Supported by an Erwin Schrödinger Fellowship of the Austrian Science Fund. Present address: Dept. of Dermatology, Medical University of Vienna, 1090 Vienna, Austria.

[3] To whom correspondence should be addressed: Harvard Medical School, Chief, Laboratory of Immunobiology and Cancer Vaccine Center, Dana Farber Cancer Institute, HIM 419, 4 Blackfan Circle, Boston, MA 02115. Tel.: 617-632-3412; Fax: 617-632-3351; E-mail: ellis_reinherz@dfci.harvard.edu.

[4] The abbreviations used are: HPV, human *Papillomavirus*; CTL, cytotoxic T lymphocyte; PBMC, peripheral blood mononuclear cells; pMHC, a complex of a peptide and an MHC molecule; TCR, T cell receptor; Rb, retinoblastoma; HTLV, human T cell leukemia virus; SFU, spot-forming unit.

specific antigens are derived from normal or mutated endogenous self-proteins (15) (TANTIGEN: Tumor T cell Antigen Database), E6 and E7 are foreign viral antigens. These two proteins are required for the induction and maintenance of the malignant phenotype of high-risk HPV-associated cancer cells (5, 6), and because HPV uses the cellular DNA replication machinery for genome synthesis, the mutation rate of HPV proteins is low. Thus, it is unlikely that HPV will evade immune attack through loss or mutation of the E6 and/or E7 gene products (16).

Studies on therapeutic vaccines, therefore, have mostly focused on E6 and E7 as target antigens. To date these targets have been delivered as naked DNA vaccines, with recombinant viral or bacterial vectors, as protein or peptide vaccines, and as fusion constructs with toll-like receptor agonists or proteins that enhance antigen delivery or presentation (for review, see Refs. 13, 17, and 18). Most clinical studies have been performed using DNA vaccines. These include a DNA HPV-16 E7 vaccine that has been tested with various fusion partners to enhance antigen presentation and with another DNA vaccine encoding E6 and E7 peptides from HPV-16 and -18 (for review, see Ref. 19). Live viral vectors also have been tested in the clinic, with vaccinia virus constructs coding for either bovine *Papillomavirus* E2 (20, 21) or HPV-16 and -18 E6 and E7 (22). As for protein vaccines, a fusion protein of heat shock protein 65 with HPV-16 E7 has been tested in three phase II trials (23–25). In addition, a fusion protein of HPV-16 E6, E7, and L2 was also in a phase II trial (26), and a HPV-16 E7 fusion protein with a *Haemophilus influenza* protein or HPV-16 E6 and E7 were applied in phase I trials in various adjuvants (13, 27). Such studies, however, have yielded disappointing clinical responses.

For induction of HPV-specific T lymphocytes in a focused manner, vaccination against defined epitopes is an attractive option. Indeed, various MHC class I-restricted CTL epitopes of HPV-16 E6 and E7 have been tested in early phase clinical studies (28–34). Nonetheless, little or no benefit over historic controls has been observed. Recently, multiple long synthetic peptide fragments of E6 and E7 have been used to create a polyepitope vaccine, which when tested in patients with HPV-16-positive vulvar intraepithelial neoplasia, exhibited promising clinical efficacy (35). This type of vaccination-induced clinical response has been the most efficacious to date and argues that a robust outcome can be engendered by peptides in conventional adjuvants.

One of the key practical challenges to specific epitope-based vaccines to stimulate cytotoxic T lymphocytes stems from the fundamental nature of T cell receptor (TCR)-based recognition. TCR recognition is referred to as MHC-restricted as, unlike antibody-based recognition, a TCR physiologically interacts with a peptide in complex with an MHC molecule (pMHC) (for review, see Refs. 36 and 37). Further complexity to TCR-based recognition is that a given peptide binds to some but not all MHC molecules. Each human being expresses 3–6 MHC class I molecules (so-called HLA molecules) and at least as many MHC class II molecules. More than 3000 variants of human MHC class I and 1000 variants of MHC class II have been characterized throughout the world to date (38). Cytotoxic T cell recognition of foreign protein antigens occurs via short (generally 9–10 amino acids long) peptides produced through proteolytic cleavage in the cytoplasmic proteasome complex. These are subsequently transported into the endoplasmic reticulum, bound to MHC class I molecules and ultimately displayed on the cell surface as a pMHC. The viral pMHC serves as a flag to target an infected or transformed cell for destruction by a CTL.

Bioinformatic approaches are important tools for peptide-based vaccines and immunotherapy. Computational methods now offer accuracies that are useful in reducing the number of potential candidate peptides that must be tested experimentally for binding to a given MHC allele (39–41). *In silico* methods cannot predict, however, which MHC class I-binding peptides are actually processed and displayed on a cell surface. We have developed an MS^3 Poisson detection mass spectrometry approach to directly assess the physical presence of predicted CTL target epitopes on tumors and infected cells. Our "predict/detect" method achieves sensitivities comparable with that of a T cell with a dynamic range of one peptide among 100,000 pMHCs displayed per cell.

Here for the first time we have interrogated the MHC class I peptide array of several HLA-A*0201 HPV-16-transformed epithelial tumor cells for the presence of any and all predicted HLA-A*0201-binding E6- and E7-derived peptides. Among E6 and E7 proteins, only a single 9-mer epitope was found on all HPV-16 transformants tested. This conserved peptide, termed $E7_{11-19}$, is predicted to have the capacity to bind to the vast majority of globally distributed A2 alleles (100 of 116 HLA-A2 alleles). We suggest that the lack of prior clinical effectiveness of targeted CTL epitope vaccination (32) is a consequence of misidentification of peptides displayed on tumor cells because of the use of indirect immunological surrogates (killing, proliferation, cytokine production, etc.) to judge T cell epitope expression. Our results offer a direct path to select allele-specific targets that should afford tumor protection to a broad population of patients.

EXPERIMENTAL PROCEDURES

Cell Lines—Three HLA-A*0201-positive, HPV-16-positive human cervical carcinoma cell lines and two cell lines transfected with HPV-16 E6 and E7 were used in this study (Table 1). CaSki (ATCC CRL-1550, HPV-16 genome integrated) was grown in DMEM (Sigma) supplemented with 10% FCS, 1% L-glutamine, and 1% penicillin/streptomycin. Cell lines C66-3 (HPV-16 genome integrated) and C66-7 (HPV-16 genome episomal) were kindly supplied by John H. Lee (Dept. of Otolaryngology, University of Iowa) and grown in E media consisting of 3:1 DMEM:Ham's F-12 supplemented with 10% FCS, 1% penicillin/streptomycin, 10 μg/ml epidermal growth factor, 10 mg/ml insulin, 25 mg/ml transferrin, 25 mg/ml hydrocortisone, 200 μg/ml tri-iodo-thyronine, and 250 μg/ml cholera toxin (42). The two transfected cell lines, N/E6E7 and OKF6/E6E7, were kindly supplied by James G. Rheinwald (Dept. of Dermatology and Harvard Skin Disease Research Center, Brigham and Women's Hospital and Harvard Medical School) and grown in K-SFM (Invitrogen).

In Silico Prediction of Potential T Cell Epitopes of HPV-16 Proteins E6 and E7—Predictions of HLA-A*0201-binding peptides (both 9-mers and 10-mers) were calculated by the three best predictive servers as described previously (43), namely the Immune Epitope Data base and Analysis Resource server, the NetMHC 3.0 server, and the NetMHCpan 2.2 server. The average predicted IC_{50} was calculated, and peptides were ranked accordingly. The 21 peptides considered in this study were synthesized by SYNBIOSCI (Livermore, CA). HPLC analysis showed that the purity of the synthesized peptides was >95%. All peptides had expected masses as confirmed by mass spectrometry. Peptides were reconstituted in DMSO at 100 μM each.

*HLA-A*0201 Binding Assay*—HLA-A*0201-positive, TAP-deficient T2 hybridoma cells (ATCC) were plated at a density of 10^6 cells/ml in 24-well plates. Cells were pulsed with 10 μM HLA-A*0201-restricted HPV-16 peptides or with 10 μM HLA-A*0201-restricted HTLV-TAX_{11-19} (LLFGYPVYV)-positive control peptide and 5 μg/ml β2-microglobulin (BD Biosciences) for 6 h at 37 °C in serum-free AIM V media (Invitrogen). HLA-A*0201 expression was determined by flow cytometry (FACSAria) using FITC-conjugated BB7.2 mAb (BD Biosciences). Mean cell fluorescence intensities (MFI) were normalized to the HTLV-TAX-positive control peptide using the formula $(MFI_{sample} - MFI_{control})/(MFI_{HTLV\text{-}TAX} - MFI_{control})$.

Interferon γ (IFNγ) ELISpot Assay—CD8$^+$ T-cell responses to the 10 HPV-16 peptides that were found to be binders in the HLA-A*0201 binding assay were quantified by IFNγ ELISpot assay. Peripheral blood mononuclear cells (PBMC) isolated from six HLA-A*0201-positive healthy donors under Institutional Review Board approval were plated at 200,000 per well with peptides at a final concentration of 10 μM in anti-IFNγ mAb 1-D1K (Mabtech, Cincinnati, OH)-coated polyvinylidene 96-well plates (Millipore, Billerica, MA). For each individual peptide, the assay was run in duplicate. A HLA-A*0201-restricted HIV-1 peptide (LTFGWCFKL-HIV/$Nef_{137-145}$) was used as a negative control, and a CMV/EBV/influenza peptide mix (CEF Peptide Pool Classic, Cellular Technology Ltd., Cleveland, OH) and phytohemagglutinin as positive controls. Secreted IFNγ was detected by biotin-labeled anti-IFNγ mAb 7B6–1, and the reaction was developed with streptavidin-ALP and the color reagent nitro blue tetrazolium/5-bromo-4-chloro-3-indolyl phosphate (Sigma). The number of specific IFNγ-secreting T cells was determined with an automated ELISpot reader, calculated by subtracting the average negative control value, and expressed as the number of spot-forming units (SFU) per 10^6 input cells. A response was considered positive if the activity was at least three times as great as the mean background activity. Of note, three of these six donors tested for HPV-16 antibody scored positive (data not shown).

Nanoscale Immune-affinity Purification by Immunoprecipitation—For each immunoprecipitation, 10 μg of anti-HLA-A02 BB7.2 mAb (BD Biosciences) was non-covalently coupled to 20 μl of Gamma Bind beads (GE Biosciences) for 1 h at room temperature. Tumor cells were harvested during the log growth phase and washed with PBS. Cells were pelleted, and the washed and dried cell pellet was lysed using 1.5 ml of lysis buffer consisting of 20 mM Tris, pH 8.0, 1 mM EDTA, 100 mM NaCl, 1% Triton X-100, and 60 mM *n*-octylglucoside (protease inhibitor tablet, Roche Applied Science, and phenylmethylsulfonyl fluoride) for 10 min on ice. Cell debris was removed using centrifugation for 30 min at maximum speed (13,000 rpm) at 4 °C. Cleared supernatant was incubated with 20 μl of antibody coupled Gamma Bind Plus beads for 2–3 h at 4 °C. Beads were washed 4 times using lysis buffer without Triton X-100 and protease inhibitors. Beads were further washed 4 more times with 10 mM Tris pH v8.0. Dried bead-antibody-HLA pellets were stored at −80 °C for a brief period before MS analysis. Peptides were recovered with 10% acetic acid followed by C18 reverse phase extraction and analyzed on MS.

MS^3 Poisson Detection Mass Spectrometry—Mathematical details, Poisson scoring, confidence estimation, numerical sampling, and other general principles of MS^3 detection are described in a separate manuscript with an analytical focus.[5] Nanospray MS^3 detection uses a hybrid quadrupole filter, collision cell, and a linear ion trap mass spectrometer (MDS Sciex QTrap 4000). In nanospray MS^3 detection a complex mixture is analyzed for a limited number of molecular targets. In place of chromatographic separations, a combination of selective isolations and dissociations filters out a fraction of the ion current highly enriched in fragments specific to a target molecule. This fraction is identified against a background of other ion fragments by using a probabilistic measure. MS^3 X/Y spectra are generated by first selectively transmitting a narrow *m/z* window centered at X into a cell where it dissociates by collision activation. The fragments collect in a linear ion trap downstream of the collision cell. After a collection period, an *m/z* window centered at Y is isolated in the linear ion trap, and the ion fragments at *m/z* Y are again dissociated by collision activation. These fragments of a fragment are scanned out and measured to create an MS^3 spectrum. For targeted detection, MS^3 spectra of synthetic versions are first studied for optimal conditions and MS^2 fragment choices, and then reference MS^3 spectra are acquired for each of the chosen MS^2 fragments. Sample MS^3 spectra with corresponding *m/z* windows and dissociation conditions are acquired, and these spectra are compared against the set of reference spectra using a Poisson probability metric to quantify the likelihood that the experimental spectra contain fragment intensities consistent with the relative arrival rates given by the reference spectra (44).[5] In contrast to chromatographic separations, the different ionizable components are simultaneously present in the ion beam. This means molecular abundance of a target can be measured by use of an added calibrant molecule at known concentration. This is done in two steps. In the first step one measures a solution with known target and calibrant concentrations to relate the MS^3 ion flux of the target to the calibrant in the detection spectra. For example, to quantitate $E7_{11-19}$, known amounts of this and a control peptide P (KSPWFTTK) are added to a mock MHC I workup using 1.2 pmol of β-galactosidase digest as a carrier. After C18 trapping and elution into the electrospray buffer, the detection MS^3 spectra of both peptides is taken in an alternating series to compensate for time variation in the nanospray ion flux. The

[5] B. Reinhold, D. B. Keskin, and E. L. Reinherz, submitted for publication.

MS^3 signal amplitudes of P (base peak at *m/z* 597.4) and $E7_{11-19}$ (base peak at *m/z* 634.4), corrected for relative amounts, are recorded. As noted in Fig. 8*A*, after a 2-min MS^3 collection for $E7_{11-19}$ at 9 fmol/μl in the β-galactosidase sample, one measures a signal amplitude of 10^7 (arbitrary units) for *m/z* 634, whereas P at 10 fmol/μl gives 7.5×10^6 for *m/z* 597. This gives the relative molar MS^3 signal response of P to $E7_{11-19}$ at about 0.68. In the second step a known amount of the calibrant peptide is added to the sample being quantitatively analyzed for target. For $E7_{11-19}$ quantitation in 10 million CaSki cells, 40 fmol of KSPWFTTK is added to the sample at the beginning of the acid elution step. The detection MS^3 spectra of peptide P and $E7_{11-19}$ is again taken in alternating sequence. The measured ratio of MS^3 ion flux for $E7_{11-19}$ and P in the CaSki sample is $2 \times 10^5/1.3 \times 10^7$ (*m/z* 634.4/*m/z* 597.4). Corrected for the molar response (0.68) as determined in the first step, one has the relative molar amounts of $E7_{11-19}$ to P in the sample as 0.0105. As 40 fmol of P was added, this gives the amount of $E7_{11-19}$ as 422 amol or 254 million molecules from 10 million CaSki cells. As the nanospray ion source often shows significant intensity variations with time and MS^3 spectra may be collected for long periods, quantitation data are always collected in a series where a single scan of the target alternates with a single scan of the calibrant and the respective scans are then summed.

Generation of HPV-16-specific T Cell Lines—For use as antigen-presenting cells, dendritic cells were differentiated from adherent donor monocytes in DMEM medium supplemented with 10% human serum, 1% L-glutamine, 1% penicillin/streptomycin, 100 ng/ml granulocyte-macrophage colony-stimulating factor, and 50 ng/ml IL-4 (PeproTech, Rocky Hill, NJ) for 1 week. Differentiated dendritic cells were matured with 10 ng/ml TNF-α, 10 ng/ml IL-6, 10 ng/ml IL-1β, 1 μg/ml prostaglandin E2, and 1 μg/ml peptidoglycan (Sigma) overnight. Cells were pulsed with 10 μM HPV-16 peptides for 3 h and irradiated (3000 radians). Fresh donor PBMC were prepared by Ficoll-Paque (Amersham Biosciences) centrifugation. Donor PBMC were plated at a density of 10^7cells/ml together with 5×10^4/ml HPV-16 peptide-loaded irradiated antigen-presenting cells in 24-well culture plates in DMEM medium supplemented with 10% human serum, 1% L-glutamine, 1% penicillin/streptomycin, 0.05 mM 2-mercaptoethanol, and 10 ng/ml IL-7. Cultures were fed with 20 IU/ml IL-2 (BD Biosciences) 5 days after stimulation and re-stimulated with peptide-loaded-irradiated donor dendritic cells every week for a total of 4 weeks.

T Cell Proliferation Assay—5×10^5 T cells from the $E7_{11-19}$-specific T cell line were stimulated with 1×10^5 donor B cells loaded with 10 μg/ml $E7_{11-19}$ on 96-well plates. Donor B cells were obtained through stimulation of donor PBMC with 3T3-CD40L cells as described previously (45). CD40-activated B cells were irradiated at 3200 rads before plating. Cells were plated in DMEM medium supplemented with 10% human serum, 1% L-glutamine, 1% penicillin/streptomycin, and 0.05 mM 2-mercaptoethanol. Plates were incubated in a 37 °C tissue culture incubator for 3 days and pulsed with 1 μCi of [^{3}H]thymidine for 16 h. Plates were harvested, and [^{3}H]thymidine incorporation was detected with a liquid scintillation mixture (PerkinElmer Life Sciences Beta Plate Scint) in a luminescence counter (PerkinElmer Life Sciences 1450 LSC).

Analysis of IFNγ Secretion Associated with HPV-16-specific Proliferative Responses—IFNγ quantitation was performed using cytometric bead arrays (BD Biosciences) according to the manufacturer's instructions. Cut-off values were based on the standard curve for IFNγ (100 pg/ml). Antigen-specific cytokine production was defined as a cytokine concentration above cut-off level and $>2\times$ the concentration of the medium control.

Characterization of T Cell Lines by IFNγ ELISpot—5×10^4 T cells from the $E7_{11-19}$-specific T cell lines were incubated with 1×10^4 T2 cells loaded with 10 μg $E7_{11-19}$ peptide overnight on precoated IFNγ ELISpot plates. The assay was processed and developed as described above.

Cytotoxicity Assay—Donor B cells from an EBV-immortalized B cell line (Laz 509) were pulsed with 10 μg or 10 ng of the respective HLA-A*0201-restricted HPV-16 peptides at 37 °C overnight. The cells were washed twice with DMEM and pulsed with 100 μCi/ml ^{51}Cr for 90 min at 37 °C. Target cells were washed three times with serum-free Opti-MEM media (Invitrogen) to remove excess ^{51}Cr and plated with peptide-specific $CD8^+$ T cells at 30:1, 10:1, 3:1, and 1:1 ratios. After 4 h of incubation, 50 μl of culture supernatant were mixed with liquid scintillation mixture (PerkinElmer Life Sciences Optiphase Supermix) and analyzed for ^{51}Cr release using a luminescence counter (PerkinElmer Life Sciences 1450 LSC). Percent specific chromium release was calculated using the formula (experimental release − spontaneous release)/(maximum release in 5% Triton X-100 − spontaneous release) × 100.

RESULTS

In Silico Prediction of Potential T Cell Epitopes of HPV-16 Proteins E6 and E7—HPV is a small non-encapsulated DNA virus containing ~8000 bp encoding two major sets of genes (E, early region genes; L, late region genes) that infect stratified squamous epithelium (Fig. 1). As the E6 and E7 proteins bind host regulators of keratinocyte cell division and thereby degrade and/or perturb the cell cycle inhibitors p53 and Rb, respectively, those viral proteins are of keen target interest for immunotherapeutic purposes. Human cell lines transformed by HPV-16 (CaSki, C66-3, and C66-7) or transduced with HPV-16 E6 and E7 containing retroviruses (N/E6E7 and OKF6/E6E7) are listed in Table 1.

Potential HLA-A*0201-binding peptides derived from the HPV-16 E6 and E7 proteins were determined using three prediction servers (Immune Epitope Data base and Analysis Resource, netMHC, and netMHCPAN) previously found to provide the most accurate HLA-A*0201 results (43). Predicted peptides were ranked by average predicted IC_{50} values as reported in Table 2. When available, experimentally determined IC_{50} measurements were also included (46). Any peptide containing more than one cysteine residue was excluded from the list to minimize complexities resulting from intramolecular or intermolecular disulfide bond formation. As shown, predictions correlated quite well with published experimental data as all top ranked peptides have been previously defined as binders, aside from peptide $E7_{12-20}$ (46). Within the top group, peptide $E7_{11-19}$ was predicted to be the best binder, whereas peptide $E7_{86-93}$ was experimentally determined to bind most strongly to HLA-A*0201 (46).

*HLA-A*0201-binding Assay*—To measure the binding capabilities of predicted peptides, an HLA-A*0201 binding assay was performed using the T2 cell line (47, 48). This cell line is TAP1/2-deficient, displaying low levels of HLA-A*0201 on its surface. After exogenous addition of peptides capable of binding to HLA-A*0201, this HLA complex is stabilized on the surface with a concomitant increase in the number of HLA-A*0201 molecules, as determined by mean fluorescence intensity staining using a fluorochrome-labeled anti-HLA-A2 antibody and flow cytometry. Binding was calculated relative to a known strong HLA-A*0201 binder, the TAX_{11-19} peptide from the human T cell leukemia virus-1 (HTLV-1). As shown in Fig. 2, peptide $E7_{86-93}$ was found to be the best binder in this assay followed by $E7_{11-19}$. Altogether, the top-ranked predicted peptides were the strongest binders in the T2 assay so that with the exception of $E7_{12-20}$, the peptides with a predicted average IC_{50} of >500 nM were not found to bind to HLA-A*0201 in the T2 assay. The T2 assay results correlated well with the previously published data (46). Those 10 peptides that were determined to bind experimentally were included in further assays.

IFNγ ELISpot Assay—Current epidemiological data suggest that virtually all individuals among the sexually active population have

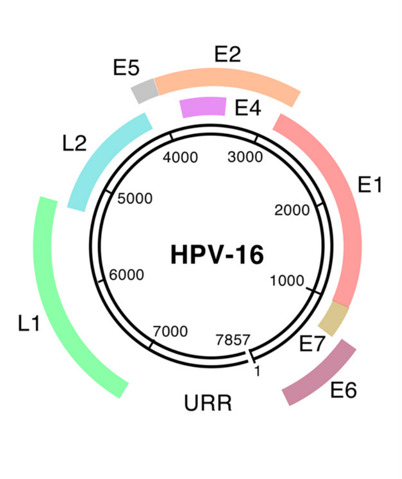

Gene	Function
L1	Major capsid protein.
L2	Minor capsid protein.
E1	Transcription factor, helicase activity. Mediates episomal DNA replication.
E2	Transcription factor. Regulates viral copy number.
E4	Facilitates virion release.
E5	Stimulates cell proliferation and prevents differentiation. Downregulates surface MHC class I expression.
E6	Deregulates cell cycle control through p53 inactivation/degradation. Induces malignant transformation together with E7.
E7	Keeps cells active in the cell cycle through Rb inactivation. Induces malignant transformation alone and together with E6.

FIGURE 1. **HPV-16 genome and transforming activity of E6 and E7.** The *left panel* shows the ~8000-bp map of this oncogenic DNA virus and its genes. In the *right panel*, the key functions of the early and late genes are listed (5, 85–93).

TABLE 1

HPV-16 transformed and E6/E7 transduced cell lines

The HPV status, names, and origins of cell lines used in the current study are provided. CaSki was obtained from ATCC (CRL-1550™) and described in Pattillo (94). C66-3 and C66-7 were gifts of J. H. Lee (42), whereas N/E6E7 and OKF6/E6E7 were gifts of J. G. Rheinwald (unpublished data).

Cell lines	HPV status	Origin
CaSki	HPV-16-transformed genome-integrated	Cervical epidermoid carcinoma, small intestinal metastasis
C66-3	HPV-16-transformed genome-integrated	Cervical keratinocytes
C66-7	HPV-16-transformed genome-episomal	Cervical keratinocytes
N/E6E7	HPV-16 E6/E7-immortalized stable human skin keratinocyte cell line	Normal foreskin keratinocytes transfected with the LXSN-16E6E7 retroviral vector
OKF6/E6E7	HPV-16 E6/E7-immortalized stable human mucosal keratinocyte cell line	Normal oral keratinocytes transfected with the LXSN-16E6E7 retroviral vector

TABLE 2

Bioinformatic predictions of HPV-16 E6- and E7-derived peptides binding to HLA-A*0201

IEDB, Immune Epitope Data base and Analysis Resource server.

Peptide position	Sequence	Predicted IC_{50}				Measured IC_{50}[a]
		IEDB	NetMHC	NetMHCpan	Average	
		nM				nM
$E7_{11-19}$	YMLDLQPET	9.6	10	10.88	10.16	49
$E7_{11-20}$	YMLDLQPETT	22.7	27	28.85	26.18	46
$E7_{7-15}$	TLHEYMLDL	48.9	30	64.43	47.78	188
$E7_{82-90}$	LLMGTLGIV	30.9	99	22.85	50.92	82
$E6_{18-26}$	KLPQLCTEL	115.2	123	62.64	100.28	328
$E6_{52-60}$	FAFRDLCIV	92.0	182	153.66	142.55	130
$E6_{29-38}$	TIHDIILECV	386.0	44	67.12	165.70	494
$E7_{86-93}$	TLGIVCPI	84.4	541	318.97	314.79	7
$E7_{85-93}$	GTLGIVCPI	286.0	535	263.26	361.42	193
$E7_{78-87}$	TLEDLLMGTL	485.0	587	439.66	503.89	
$E6_{21-30}$	QLCTELQTTI	796.8	755	569.89	707.23	
$E7_{77-86}$	RTLEDLLMGT	429.7	1381	901.31	904.00	
$E6_{59-68}$	IVYRDGNPYA	1003.4	1494	761.84	1086.41	
$E7_{78-86}$	TLEDLLMGT	3079.2	422	373.13	1291.44	
$E7_{66-74}$	RLCVQSTHV	952.5	4014	514.67	1827.06	
$E6_{44-53}$	LLRREVYDFA	2592.1	1894	1462.12	1982.74	
$E7_{82-91}$	LLMGTLGIVC	590.1	4206	1668.83	2154.98	
$E6_{89-97}$	SLYGTTLEQ	3836.3	923	2746.42	2501.91	
$E7_{12-20}$	MLDLQPETT	3813.3	3103	1973.12	2963.14	462
$E7_{81-90}$	DLLMGTLGIV	398.6	6154	6013.88	4188.83	
$E6_{86-95}$	YCYSLYGTTL	1184.1	4394	7122.60	4233.57	

[a] See Ref. 46.

been exposed to HPV infection (for review, see Refs. 13 and 49 and references therein). We, therefore, examined the ability of T cells from fresh peripheral blood mononuclear cells of six HLA-A*0201-positive healthy donors to recognize these HPV candidate peptides in IFNγ ELIspot assay. As shown in Fig. 3*A*, SFUs per 10^6 cells were low or undetected in these individuals. However, when SFUs were observed, their size was substantial (Fig. 3*B*). The low numbers of IFNγ-producing cells reflect the paucity of HPV-specific memory T cells in peripheral blood. These findings are also consistent with previous studies (50) reporting low HPV-specific SFUs and distinct from the robust memory recall SFU response to CEF (a mix of cytomegalovirus, Epstein-Barr virus, and influenza A virus) peptides or the phytohemagglutinin (*PHA*) assay control (Fig. 3*B*). The only HPV peptides eliciting an SFU number 4–5-fold over background in one donor each were $E7_{11-19}$ and $E6_{29-38}$ (Fig. 3*A*). As a consequence of these equivocal responses, we pursued mass spectrometry analysis to identify which viral peptides are physically displayed on HPV-16-transformed, HLA-A*0201-positive cells.

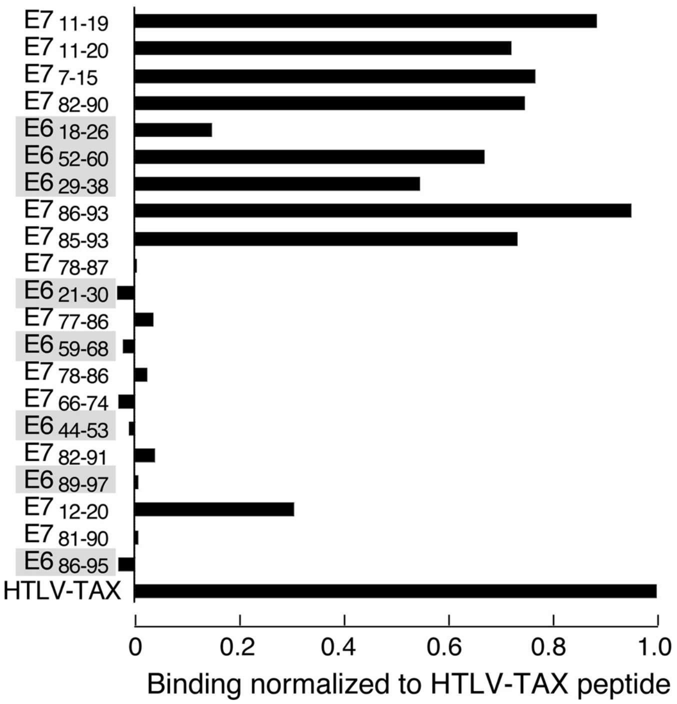

FIGURE 2. **HLA-A*0201 T2-based peptide binding assay.** HLA-A*0201-positive, TAP-deficient T2 cells were pulsed with 10 μM of the respective peptides given on the graph ordinate for 6 h at 37 °C. Binding was determined with the anti-HLA-A2 antibody BB7.2 by flow cytometry and calculated relative to a known strong binder, the TAX_{11-19} peptide from the HTLV on the *abscissa*. The TAX_{11-19} binding was set at 1.0. The order of peptides is from predicted strongest to weakest binders, *top* to *bottom*, respectively. *Shaded entries* are E6-derived peptides, whereas *unshaded entries* are E7-derived.

*HLA-A*0201 Immunoprecipitation and MS³ Analysis of Eluted Peptides*—For the investigation of HPV-16 antigen presentation by MS analysis, HLA-A*0201$^+$ HPV-16-transformed tumor cell lines as well as E6/E7 expressing human epithelial cell lines enumerated in Table 1 were used. The analytic approach employed is schematically shown in Fig. 4. In brief, tumor cells ($\sim$20–60 $\times$ 10^6) were solubilized using detergent buffers, and then HLA-A*0201 molecules were immunoprecipitated with the BB7.2 anti-HLA-A2-specific mAb coupled to Gamma Bind Plus beads. Peptides were recovered from pMHC complexes by acid elution and analyzed on a hybrid quadrupole-linear ion trap mass spectrometer using MS³ and Poisson statistics as described under "Experimental Procedures." Peptides from HPV-16 E6 and E7 oncoproteins that were shown by T2 assay to increase surface HLA-A2 expression (Fig. 2) were targeted for detection by mass spectrometry.

MS³ spectra from immunoaffinity-purified HLA-A*0201 complexes isolated from HPV-16-transformed cell lines (MS³-HLA-A2) were compared against the MS³ patterns of synthetic peptides (MS³-reference) using a probabilistic metric (44[5] as shown in Fig. 5. Unexpectedly, only one peptide, $E7_{11-19}$, was easily identified, whereas $E6_{29-38}$, the sole other peptide detected, was near the limit of sensitivity. For $E7_{11-19}$, the double-charged molecular ion was selected at *m/z* 555.3 and dissociated. The proline in $E7_{11-19}$ (YMLDLQ**P**ET) tends to direct fragmentation to the amide bond on the amino side of the proline residue. This generates a strong b_6 (YMLDLQ-) fragment at *m/z* 764.4, making an optimal candidate for MS³ detection but suppressing the detection by other fragments (supplemental Fig. S1). The molecular ion is abundant in the peptides recovered from the HPV-16-positive CaSki cervical carcinoma line so that the dissociation pattern of the b_6 fragment from the synthetic peptide is immediately recognized in the MS³ 555.3/764.3 spectrum (Fig. 5, *A* and *B*, and supplemental Fig. S3). The Poisson signature of detection (peak at 0 *m/z* shift, Fig. 5*C*) is clear cut but, in this case, largely superfluous. The b_8 fragment (YMLDLQPE-) was also detected in the MS³ 555.3/990.4 spectrum of recovered peptides (supplemental Fig. S2). In contrast to detecting the b_6 fragment of

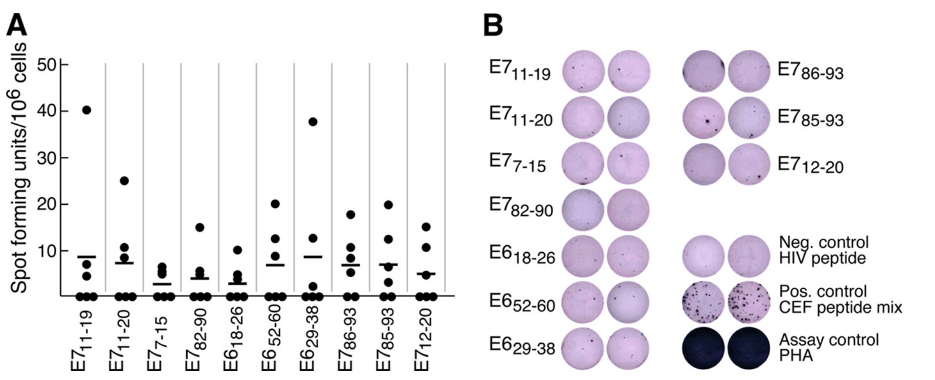

FIGURE 3. **Low or undetectable memory T cells in blood of healthy individuals.** Immune recognition of the 10 HLA-A*0201-binding peptides was tested in an IFNγ ELISpot assay. PBMC isolated from 6 HLA-A*0201-positive healthy donors were stimulated with 10 μM respective peptide overnight. In *panel A*, spots are graphed and presented as SFUs per million PBMC. SFUs of single donors are represented as *dots*, with a horizontal line corresponding to the mean of six donor samples. Highest SFUs are not from the same donor. In *panel B*, ELISpot well images from representative plates (2 $\times$ 10^5 cells/well) taken from several donors are shown. *CEF*, cytomegalovirus/Epstein-Barr-Virus/Influenza positive peptide mix. *PHA*, phytohemagglutinin, a mitogenic plant lectin used as another positive control.

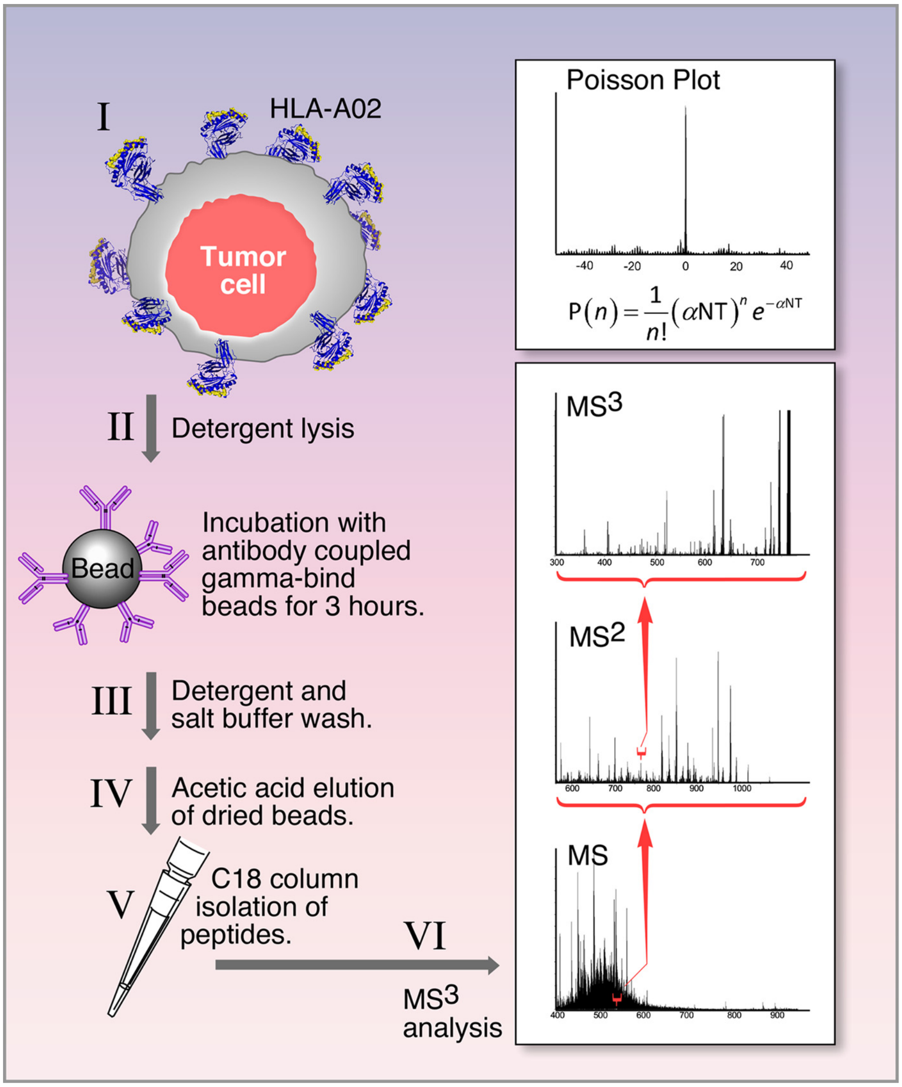

FIGURE 4. **Methodology for immunoprecipitation of HLA-A2 molecules, elution of bound peptides, and MS^3 analysis of potential CD8 T cell epitopes.** MS^3 analysis isolates a selected *m/z* window containing a target ion (*e.g. m/z* 555.3), fragments (by collision activation) all ions in the selected window, isolates from these fragments a second *m/z* window containing a target fragment (*e.g. m/z* 764.3), and dissociates ions in the second *m/z* window to form an MS^3 spectrum (denoted MS^3 555.3/764.4). A probabilistic measure quantifies the likelihood the MS^3 spectrum generated in these steps contains a reference dissociation pattern obtained from the synthetic peptide. Details are provided under "Experimental Procedures."

$E7_{11-19}$, detection of $E6_{29-38}$ by MS^3 fragmentation of the b_8 ion (TIHDIILE-) at *m/z* 935.5 (MS^3 578.3/935.5; Fig. 5, *G–I*) is not so evident by inspection of the MS^3 spectra (Fig. 5, *G* and *H*) but does produce the detection signature using the Poisson metric (Fig. 5*I*). $E6_{29-38}$ detection was further supported by a similar Poisson analysis for the signature of the b_7 ion (TIHDIIL-) at *m/z* 806.5 (data not shown).

The longer $E7_{11-20}$ peptide has received considerable attention in the literature as a possible tumor antigen (32), but it was not detected on CaSki (Fig. 5, *D–F*) nor on any other E7 expressing cell line. MS^3 analysis of synthetic $E7_{11-19}$ and $E7_{11-20}$ peptides showed equivalent signal intensity in generating the MS^3 spectra used for detection, and both peptides were recovered equivalently from peptide-loaded T2 cells (data not shown). Nonetheless, the difference in surface presentation between $E7_{11-19}$ and $E7_{11-20}$ peptides was substantial. Processing 60 million CaSki cells and MS^3 analysis of $E7_{11-19}$ and $E7_{11-20}$ produced a Poisson amplitude of almost 700 events for the $E7_{11-19}$ peptide, whereas the $E7_{11-20}$ detection under identical conditions did not rise above background (10 events).

*MS^3 Detection Analysis Identifies $E7_{11-19}$ on All HPV-16-expressing HLA-A*0201$^+$ Human Epithelial Lines*—Poisson detection signatures of $E7_{11-19}$ were obtained from each of the human cell lines described in Table 1. As shown in Fig. 6, from 10–20 × 10^6 C66-7, OKF6/E6E7, N/E6E7, C66-3, and CaSki cell lines, the HLA-A*0201-bound $E7_{11-19}$ peptide was readily observed by MS^3 Poisson detection mass spectrometry (*panels A–E*, respectively). In contrast, calculating the Poisson signature of the $E7_{11-19}$ b_6 fragment against 10 representative MS^3 ion backgrounds did not indicate a single instance of positive detection (supplemental Fig. S4). Furthermore, as shown by quantitative flow cytometry analysis of HLA-A2 expression using the anti-HLA-A2 mAb BB7.2, the fraction of surface display due to this epitope is enhanced, as the total HLA-A*0201 copy number is reduced >10-fold on these HPV-16-transformed or -transfected cells relative to the TAP competent T1 cell line or EBV-transformed B cell line Laz 509. Their levels of MHC class I expression are more similar to the TAP-deficient T2 cell line than the TAP-sufficient Laz 509 or T1 cells (Fig. 6*F*). However, unlike T2 cells, the HPV-16 epithelial cell MS spectra are not dominated by signal peptides of normal proteins (51). In summary, cervical and oral epithelial cells displayed detectable surface HLA-A*0201-bound $E7_{11-19}$ after HPV-16 infection or ectopic expression of HPV-16 gene products. On the other hand, aside from $E6_{29-38}$ in CaSki cells (Fig. 5), MS^3 detected no other E6 or E7 epitopes with HLA-A*0201 binding activity as observed in the T2 assay (data not shown).

Unexpectedly, the peptide recovery as characterized by mass spectrometry from the C66-7, N/E6E7, and OKF6/E6E7 lines compared with the recovery from the C66-3 and CaSki lines was substantially lower than the amount expected from comparing HLA-A2 expression by flow cytometry. The reason for this is currently under study, but the large variation in overall recovery is best addressed by a direct method of comparing the relative fraction of $E7_{11-19}$ to total peptide among the different cell lines. Such a measure can be obtained from the MS^2 555.3

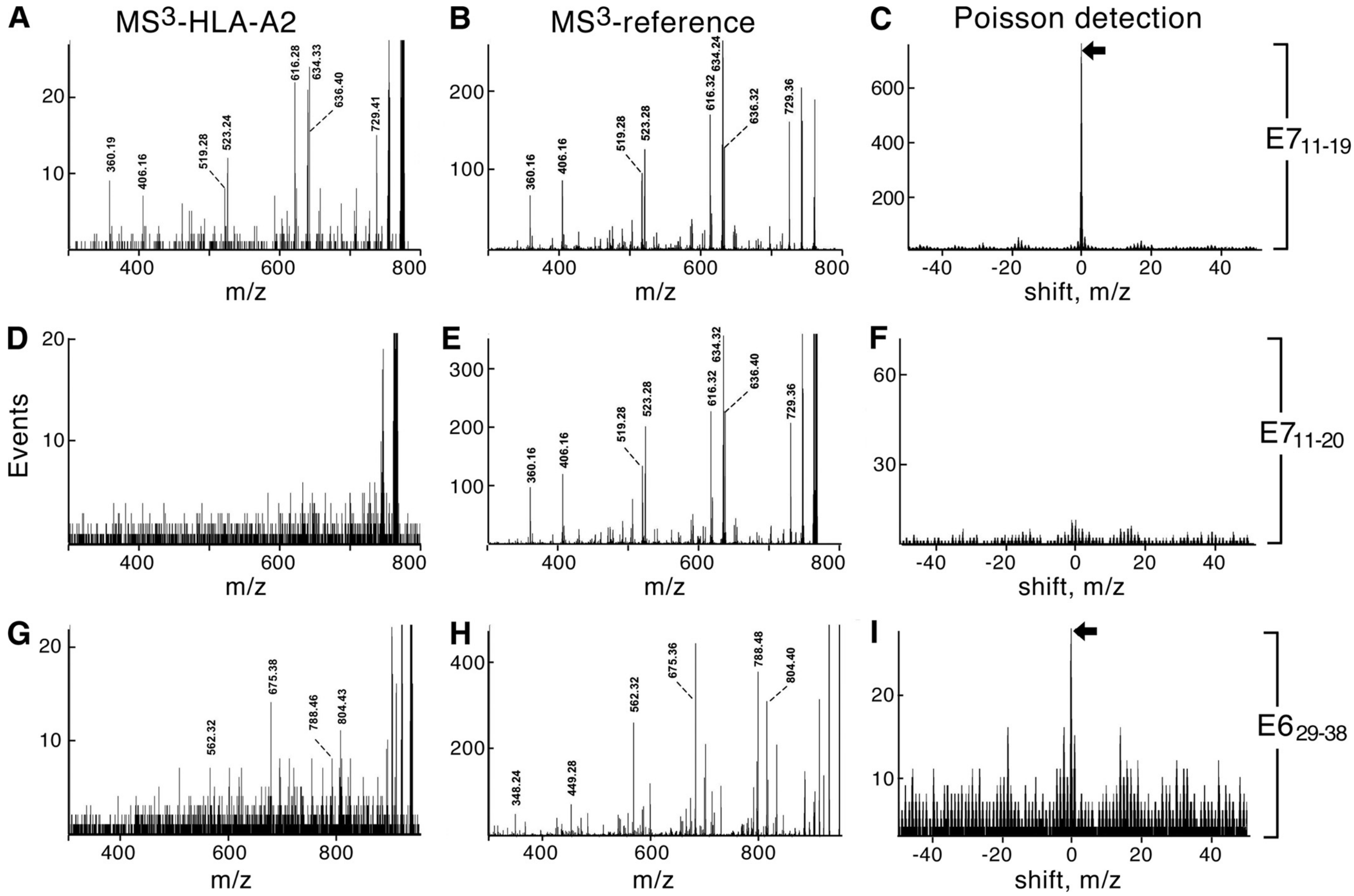

FIGURE 5. **MS^3 detection analysis of $E7_{11-19}$, $E7_{11-20}$, and $E6_{29-38}$ HPV-16 peptides.** Comparison of MS^3-HLA-A2 extracts with MS^3 reference patterns is shown in the *left* and *middle columns*, respectively. Poisson detection signatures are shown in the *right columns*. *A*, MS^3 555.3/764.4 of HLA-A2-associated peptides extracted from 60 million CaSki cells is shown. *B*, MS^3 555.3/764.4 of synthetic peptide YMLDLQPET corresponding to $E7_{11-19}$ is shown. *C*, shown is the Poisson detection signature of the synthetic pattern shown in *B* in the spectrum shown in *A*. The amplitude at 0 *m/z* shift relative to nonzero *m/z* shifts is a probabilistic measure of the uniqueness of the fit and is used as a marker of detection (see "Experimental Procedures" and "Results" sections). *D*, MS^3 605.8/764.4 of HLA-A2 peptides extracted from 60 million CaSki cells is shown. *E*, MS^3 605.8/764.4 of synthetic peptide YMLDLQPETT corresponding to $E7_{11-20}$ is shown. *F*, the Poisson detection signature of the b_6 fragment (YMLDLQ-) is shown. *G*, MS^3 578.3/935.5 of HLA-A2-associated peptides extracted from 20 million CaSki cells is shown. *H*, a reference spectrum of the b_8 fragment (TIHDIILE)- from MS^3 578.3/935.5 of the synthetic peptide TIHDIILECV is shown. *I*, Poisson detection signature of the b_8 fragment in MS^3 578.3/935.5 spectrum of peptides extracted from CaSki cells is shown.

spectra (Fig. 7). These spectra show a number of intense shared peaks at the high *m/z* end that arise from common terminal losses. Different peptides with molecular masses near 1108.6 Da are co-selected as double-charged ions in the *m/z* 555.3 window, and if these ions lose a common amino acid residue at the amino or carboxyl terminus, their product ions will appear as a single *m/z* peak. For example, *m/z* 992.6, 978.6, 949.5, and 859.5 could be b-type ions that arise from the carboxyl-terminal loss of Val, Leu or Ile, Ala-Ala, and (Leu or Ile)-Glu, respectively. The peak at *m/z* 978.6 could be a y-type ion arising from the amino-terminal loss of methionine and so on. Because these high *m/z* peaks reflect the contribution of many peptides, their collective intensity is a qualitative measure of the peptide background. In contrast the peak at *m/z* 764.4 that appears above the background in the C66-3-, CaSki-, and $E7_{11-19}$-loaded Laz 509 B cell line spectra is shown by MS^3 to be predominantly a fragment of the $E7_{11-19}$ peptide. The ratios of *m/z* 764.4 to the peaks at *m/z* 992.6, 978.6, 949.5, and 859.5 (Fig. 7) are a relative measure of the $E7_{11-19}$ fraction and show that the low MS^3 ion flux for the $E7_{11-19}$ peptide in the C66-7, N/E6E7, and OKF6/E6E7 lines (Fig. 6) is not just a reflection of low peptide recovery overall but that the fraction of $E7_{11-19}$ to total peptide is reduced compared with that fraction in C66-3-, CaSki-, or 10 ng/ml $E7_{11-19}$-loaded Laz 509.

To quantitate the number of $E7_{11-19}$ epitopes bound to HLA-A*0201, we developed a method using a calibrant peptide (P) whereby the MS^3 spectrum of the calibrant and $E7_{11-19}$ are taken in alternating series as described in Fig. 8 (*panels A* and *B* and the legend). Fig. 8*C* shows that CaSki cells endogenously express 25 copies of $E7_{11-19}$ per cell, whereas exogenous addition of 10 ng/ml synthetic $E7_{11-19}$ to Laz 509 loads 37 copies of this HLA-A*0201 epitope per cell.

Generation and Characterization of T Cell Lines—To next test if PBMC from an HLA-A*0201-positive donor could be activated by $E7_{11-19}$-loaded autologous dendritic cells, *in vitro* stimulation was performed. After 4 weekly stimulations, the resulting T cell lines consisted of up to 70% $CD8^+$ T cells. As shown in Fig. 9*A*, these $CD8^+$ T cells proliferated when stimulated with $E7_{11-19}$ peptide-loaded autologous CD40-activated B cells but did not proliferate against control HIV-peptide (LTFGWCFKL-HIV/$Nef_{137-145}$)-loaded CD40-activated B cells as judged by tritiated thymidine incorporation. Upon

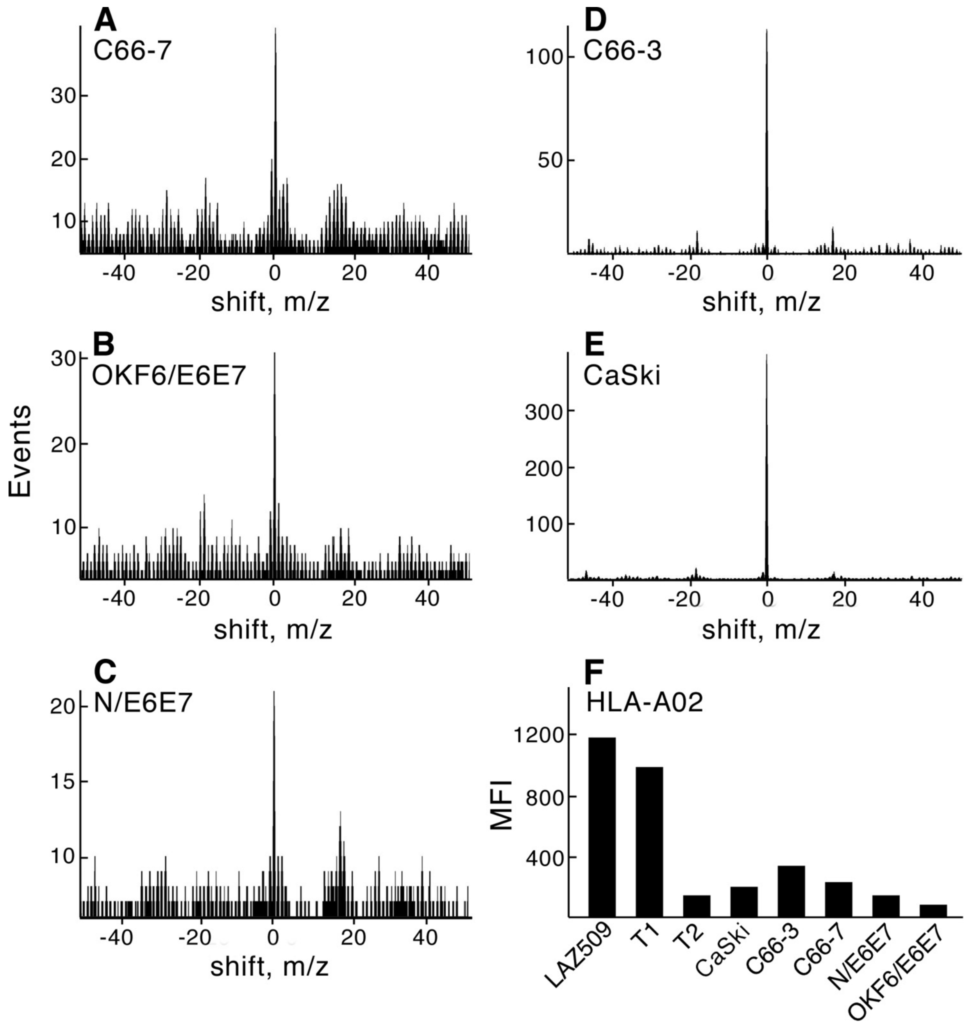

FIGURE 6. **Poisson detection of $E7_{11-19}$ on all HPV-16-transformed and -transfected human epithelial cells and their HLA-A2 surface expression.** *Panels A–E* represent Poisson detection signatures of $E7_{11-19}$ from 20 million C66-7 cells (*A*), 10 million E6/E7 transfected oral OKF6/E6E7 keratinocytes (*B*), 10 million E6/E7 transfected foreskin keratinocytes (N/E6E7) (*C*), 20 million C66-3 cells (*D*), and 20 million CaSki cells (*E*). *Panel F* shows mean cell fluorescence intensity values of the indicated cells reacting with the FITC-labeled anti-HLA-A2 mAb BB7.2.

stimulation with peptide-loaded antigen-presenting cells or T2 target cells, $E7_{11-19}$-specific T cells produced IFNγ as detected by multiplex cytometric bead array or ELISpot assay (Fig. 9, *B* and *C*, respectively). Collectively, these data show that the T cell line is specific for $E7_{11-19}$. ELISpot analysis suggested that the frequency of antigen-specific T cells in the cell line was $\geq$100-fold that detected in fresh autologous PBMC from the same donor (compare Figs. 3 and 9).

To assess whether the T cell line manifests cytolytic activity able to lyse target cells displaying a number of $E7_{11-19}$ epitopes comparable with those arrayed on CaSki, we loaded the autologous donor EBV-immortalized B cell line Laz 509 with 10 ng/ml or 10 μg/ml $E7_{11-19}$. As shown in Fig. 9*D*, $E7_{11-19}$-specific T cells lyse both $E7_{11-19}$ peptide-loaded Laz 509 target cells in a ^{51}Cr release assay. Up to 52% CTL activity was observed against 10 ng/ml $E7_{11-19}$-loaded target cells at a 30:1 E/T ratio. By contrast, no killing was observed with the same Laz 509 cells pulsed with 10 μg/ml HIV-1 peptide ($Nef_{137-145}$). These same T cells also lysed CaSki, consistent with display of $E7_{11-19}$ at equivalent density. However, given that CaSki and the T cell line differ at class I alleles other than HLA-A*0201, alloreactivity might have been, at least in part, responsible for that cytolysis (data not shown). The use of autologous B cells pulsed with $E7_{11-19}$ excludes alloreactivity as the basis for target lysis. Fig. 9*C* also indicates that whereas the T cell line raised against $E7_{11-19}$ shows specificity for $E7_{11-19}$, it lacks detectable $E7_{11-20}$ reactivity as judged by ELIspot. In a reciprocal manner, a T cell line raised against $E7_{11-20}$ showed no specificity for B cells pulsed with $E7_{11-19}$ (data not shown).

The $E7_{11-19}$ Epitope Is Highly Conserved among HPV-16 Strains and Binds to the Vast Majority of A2 Alleles—Given the expression of $E7_{11-19}$ on HPV-16 transformed or transfected cell lines, we determined whether known strains of HPV-16 conserve this epitope. Using the Human Papillomavirus T Cell Antigen Database with 791 HPV protein entries, we performed multiple sequence alignment of the 16 HPV-16 E7 sequences. As shown in Fig. 10, $E7_{11-19}$ is fully conserved in 15 of 16 sequences. A single conservative amino acid substitution is found in the remaining sequence. The latter represents a single variant among 35 HPV-16 cervical cancer or cervicitis patients analyzed. Analysis of the complete E7 open reading frame from those 35 patients revealed four nucleotide variations in three (8.5%) patients, whereas the other 32 did not contain any nucleotide changes compared with the prototype (52). Of the identified changes, two were silent nucleotide changes, and two were missense substitutions, resulting in the amino acid changes L15V and S31R. This rare LI5V conservative mutation falls within the $E7_{11-19}$ epitope.

Fig. 11, *panel A*, lists $E7_{11-19}$ HLA binding predictions on all 116 HLA-A2 alleles using NetMHCpan (53) and their calculated IC_{50} values (in nM). Significant binding is predicted for 100 of the 116 HLA-A2 alleles. As graphically depicted in *panel B*, $E7_{11-19}$ is a strong binder to 85 alleles (<50 nM), a weak binder to 15 alleles (50–500 nM), and a non-binder to 16 alleles (>500 nM).

DISCUSSION

HPV-induced dysplasia and cancer cause significant morbidity worldwide (7). Although prophylactic vaccines are now available, immunization does not reach everyone at risk. Given

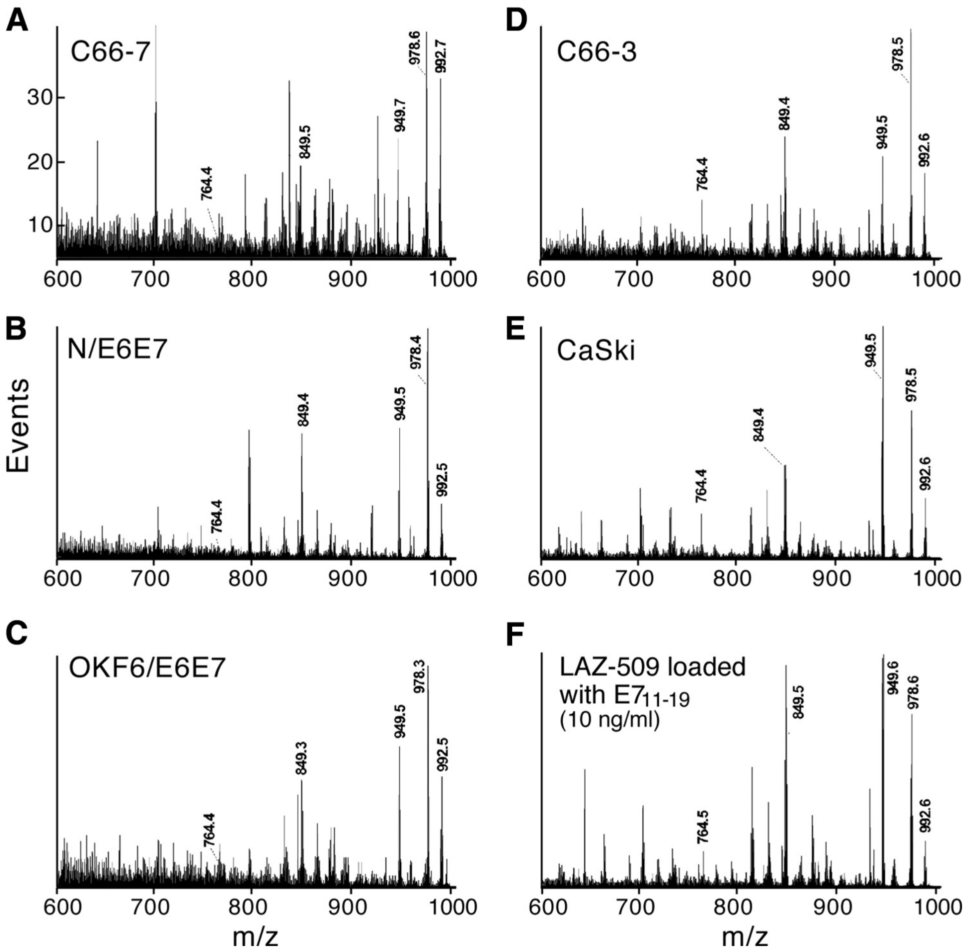

FIGURE 7. **The MS^2 555.3 spectra of HLA-A*0201 peptide extracts from different cell lines expressing the E7 oncoprotein and Laz 509 B cells loaded with 10 ng/ml E7$_{11-19}$.** The common peaks at the high *m/z* end are fragments from different peptides sharing amino or carboxyl terminal amino acids and a molecular mass near 1108.6 Da (hence, co-selected in the *m/z* 555.3 window). Because the intensity of these high *m/z* peaks is an average of many peptides, their intensity serves as an approximate measure of the peptide background. Their amplitude relative to *m/z* 764.4 provides in a single spectrum a characterization of the fraction of A2-bound peptide that is E7$_{11-19}$ (see "Results"). The C66-7, N/E6E7, and OKF6/E6E7 samples show not just lower absolute amounts of E7$_{11-19}$ (Fig. 6) but also that E7$_{11-19}$ is a smaller relative fraction of the total peptide population.

that HPV-associated cancers develop years and often decades after initial infection, it was predicted that no measurable decline of HPV-associated cancers in women may occur before 2040. This prediction was based upon higher acceptance rates for the vaccines than is currently achieved in the United States (for review, see Ref. 13). Furthermore, the approved prophylactic vaccines have no therapeutic effects (54), leaving HPV-infected individuals in need of treatment options. Fortunately, most HPV infections are cleared naturally by the immune system (14). If the lesions do not regress, surgical treatments are necessary. These procedures are associated with significant morbidity ranging from dysfunction to infertility depending on the site and stage of the lesion. A noninvasive treatment such as a therapeutic vaccine fostering an effective anti-HPV state would be an attractive alternative. A vaccine could be offered to patients who do not clear HPV infection spontaneously during a finite observation period as well as to patients with established lesions.

HPV-related diseases represent an ideal set of clinical disorders to test development of a therapeutic cancer vaccine as the viral oncoproteins E6 and E7 are consistently expressed in HPV-associated cancers (16), and they represent "non-self" cancer antigens. Given their key role in cancerous transformation, a large body of research focusing on E6 and E7 as therapeutic vaccine targets has been conducted. Multiple MHC class I- and class II-restricted epitopes, mostly of HPV-16 and HPV-18, have been reported (19, 30, 46, 55–69). Several HLA-A*0201-restricted HPV-16 E7 epitopes have already been applied in clinical trials, namely E7$_{11-20}$ (32, 33), E7$_{86-93}$ (31–34), and E7$_{12-20}$ (34). Although induction of peptide-specific T cell responses could be demonstrated in these studies, no clinical improvements exceeding the rate of spontaneous tumor regression were observed.

The lack of clinical impact was thought to be a consequence of an advanced stage of disease in the patient groups. However, as there is evidence that HPV infection influences antigen presentation, this lack of success might be caused by a paucity (or even absence) of epitopes presented on HPV-16-transformed cells. In this regard several HPV immune evasion mechanisms have been described (for review, see Refs. 70–72) including down-regulation of components of the antigen-processing machinery and MHC class I molecules (73, 74), resulting in decreased presentation of antigenic peptides. Furthermore, precise and direct identification of T cell epitopes expressed on HPV-transformed cells has been lacking. Instead, determination of relevant epitopes has been inferred by bioinformatic prediction, synthetic peptide HLA binding studies, and peripheral T cell functional activation readouts employing various immunologic assays. However, because the success of a therapeutic vaccine is dependent on accurate identification of HPV epitopes displayed as pMHC on HPV-infected target cells or HPV-transformed tumor cells, it is essential to define HPV-16 E6 and E7 T cell epitopes that are naturally processed and presented on the surface of virally altered cells. Only those HPV peptide/MHC class I complexes are capable of being recognized by cytolytic T lymphocytes to target destruction of transformed cells.

To this end, we have developed a new methodology, nanospray MS^3 Poisson detection mass spectrometry. This methodology works by filtering the ion beam through two stages of mass selection and fragmentation (generating MS^3 spectra) and detecting a target molecule by a probabilistic measure of the

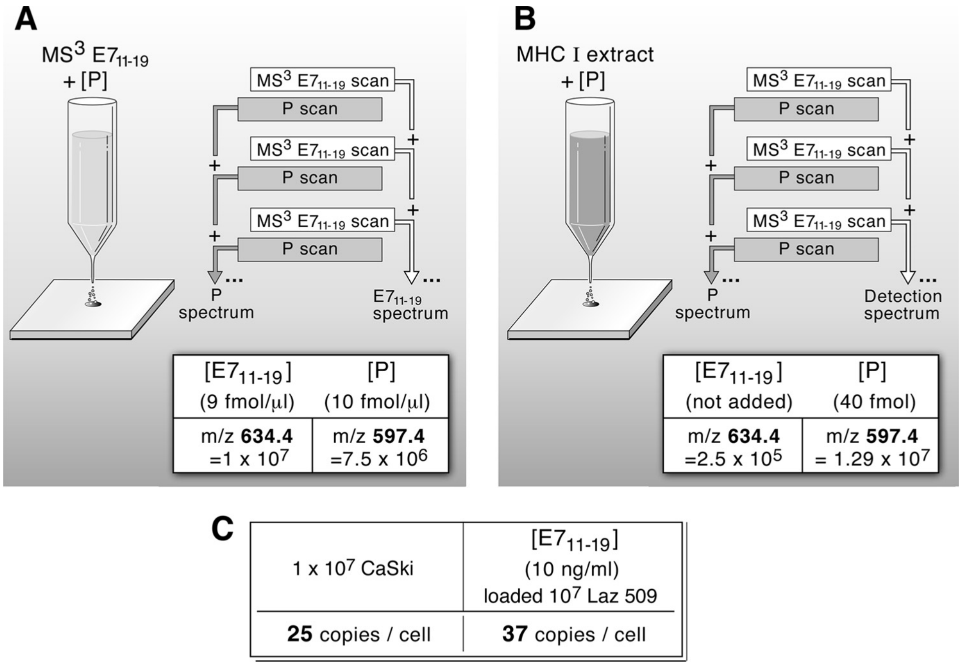

FIGURE 8. **Quantitation of the number of E7$_{11-19}$ epitopes per cell on HPV epithelial transformants and peptide-pulsed lymphoid cells.** To quantitate the amount of E7$_{11-19}$ recovered from HLA-A2 extracts, the MS^3 signal abundance relative to an added control peptide is measured. *A*, the MS^3 signals of the target E7$_{11-19}$ and control P (KSPWFTTK) peptides were measured at known concentrations in a mock MHC I workup. *B*, a known amount of the control peptide P was added to the HLA-A2 sample being analyzed, and MS^3 spectra of peptide P and E7$_{11-19}$ were again taken. *C*, combining the MS^3 signal ratios measured in A and B with the amount of control peptide added provided the amount of target peptide (see "Experimental Procedures"). Knowing the number of cells lysed, the target copies per cell were calculated assuming full recovery up to the point where the control peptide was added (Step IV, Fig. 4).

target's known dissociation patterns in the MS^3 spectra. The methodology combines instrumental and ionization optimizations in a detection mode format to provide a high dynamic range from limited sample amounts. An instrumental geometry in which a quadrupole filter is placed in front of an ion trap (QTrap 4000) achieves a high duty cycle for MS^3 spectra. Static nanospray avoids losses from surface exposure associated with chromatography and in its low (a few nanoliters per minute) flow, an optimal conversion of molecules in the condensed phase into gas phase ions.

Our findings are that none of the clinically targeted A2 peptides employed in epitope-based T cell vaccines to date could be detected on HPV-16-transformed cell lines tested herein. Two examples of this discordance are of particular note. The E7$_{86-93}$ peptide has been previously reported to be by far the best HLA-A*0201-binding peptide derived from HPV-16 (46). It is among the top predicted binders in the present study and the strongest binder in the HLA-A*0201 T2 binding assay. Nonetheless, E7$_{86-93}$ could not be detected by mass spectrometry on any of the HPV-16-transformed tumor cell lines. Furthermore, MS and fragmentation analyses of the peptides recovered from E7$_{86-93}$-loaded T2 cells showed that more than 90% of the E7$_{86-93}$ peptide complexed with HLA-A*0201 was modified with an additional cysteine that could be localized to the backbone cysteine residue and is most likely linked via a disulfide bridge (data not shown). This modification was also checked by MS^3 analysis but was not detected on an HPV-16-transformed cell line. Likewise, E7$_{11-20}$ was not present on HPV-16 human tumor cells, although E7$_{11-19}$ was rather abundant. Based on our current observations, we suggest that one reason for the lack of clinical efficacy of epitope-based therapeutic T cell vaccines for HPV-16 and, by extension, other infectious diseases and cancers may be that vaccine-elicited responses were misdirected.

The E7$_{11-19}$ 9-mer was detected on all five HLA-A*0201$^+$ HPV-16-expressing cell lines examined (Fig. 6). As shown, the amount of E7$_{11-19}$ displayed relative to other endogenous HLA-A2 bound peptides varies significantly. These differences fit well with our knowledge about integrated *versus* episomal HPV-16 genome expression (75). The two cell lines with the integrated HPV-16 genome, CaSki and C66-3, which can have no E2-induced repression of E6 and E7 expression, display relatively more E7-derived peptide on their surface. By contrast, the transformed cell line C66-7 with the episomal HPV-16 genome in which E2 is still present displays far less E7$_{11-19}$. The

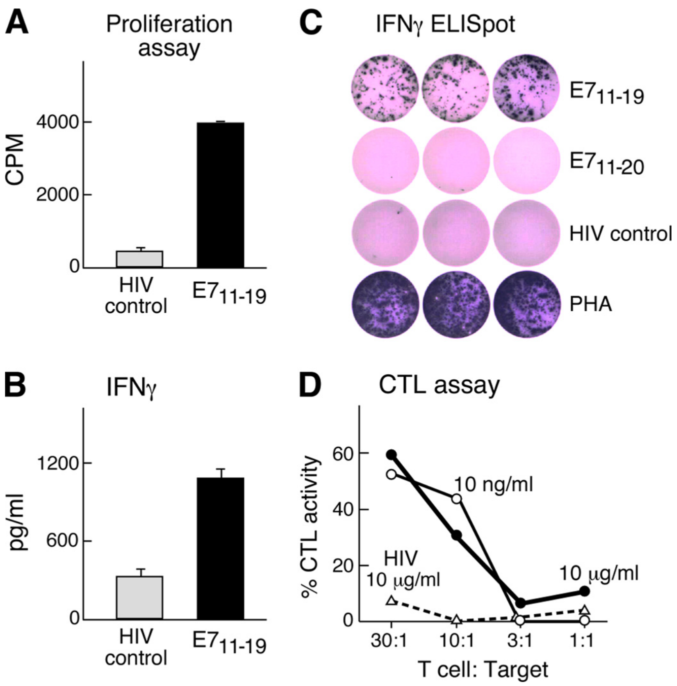

FIGURE 9. **Specificity of CD8 T cells elicited against E7$_{11-19}$ was directed against E7$_{11-19}$ but not E7$_{11-20}$.** E7$_{11-19}$-specific T cells were generated by four weekly stimulations with autologous dendritic cells and tested for their antigen-specific proliferation by tritiated thymidine incorporation (*panel A*), IFNγ secretion by cytometric bead assay (*panel B*), IFNγ production by ELISpot (*panel C*), and ability to lyse autologous EBV-transformed B cells pulsed with the indicated amounts of E7$_{11-19}$ or an irrelevant Nef$_{137-145}$ (LTFGWCFKL) HIV peptide (*panel D*). *PHA*, phytohemagglutinin.

```
A0MPS5  MHGDTPTLHEYMLDLQPETSDLYCYEQLNDSSEEEDEIDGPAGQAEPDRAHYNIVTFCCKCDSTLRLCVQSTHVDIRTLEDLLMGTLGIVCPICSQKP
A0MPS6  MHGDTPTLHEYMLDLQPETTDLYCYEQLNDSSEEEDEIDGPAGQAKPDRAHYNIVTFCCKCDSTLRLCVQSTHVDISTLEDLLMGTLGIVCPICSQKP
A0MPS7  MHGDTPTLHEYMLDLQPETTDLYCYEQLNDSSEEEDEIDGPAGQAEPDRAHYNIVTFCCKCDFTLRLCVQSTHVDIRTLEDLLMGTLGIVCPICSQKP
B7T164  MHGDTPTLHEYMLDLQPETTDLYCYEQLNDSSEEEDEIDGPAGQAEPDRAHYNIVTFCCKCDSTLRSCVQSTHVDIRTLEDLLMGTLGIVCPICSQKP
C0KXQ4  MHGDTPTLHEYMLDLQPETTDLYCYEQLNDRSEEEDEIDGPAGQAEPDRAHYNIVTFCCKCDSTLRLCVQSTHVDIRTLEDLLMGTLGIVCPICSQKP
C0KXQ5  MHGDTPTLHEYMLDVQPETTDLYCYEQLNDSSEEEDEIDGPAGQAEPDRAHYNIVTFCCKCDSTLRLCVQSTHVDIRTLEDLLMGTLGIVCPICSQKP
O11650  MHGDTPTLHEYMLDLQPETTDLYCYEQLSDSSEEEDEIDGPAGQAEPDRAHYNIVTFCCKCDSTLRLCVQSTHVDIRTLEDLLMGTLGIVCPICSQKP
O12337  MHGDTPTLHEYMLDLQPETTDLYCYEQFNDSSEEEDEIDGPAGQAEPDRAHYNIVTFCCKCDSTLRLCVQSTHVDIRTLEDLLMGTLGIVCPICSQKP
O12338  MHGDTPTLHEYMLDLQPETTDLYCYEQLNDSSEEEDEIDGPAGQAEPDRAHYNIVTFCCKCDSTLRLCVQSTHVDICTLEDLLMGTLGIVCPICSQKP
Q2MJT4  MHGDTPTLHEYMLDLQPETTDLYCYEQLNDSSEEEDEIDGPAGQAEPDRAHYNIVTFCCKCDSTLRLCVQSTHVDIRALEDLLMGTLGIVCPICSQKP
Q77GV7  MHGDTPTLHEYMLDLQPETTDLYCYEQLNDSSEEEDEIDGPAGQAEPDRAHYNIVTFCCKCDSTLRLCVQSTHVDIRTLEDLLMGTLGIVCPICSQKP
Q8QRD2  MHGDTPTLHEYMLDLQPETTDLYCYEQLHDSSEEEDEIDGPAGQAEPDRAHYNIVTFCCKCDSTLRLCVQSTHVDIRTLEDLLMGTLGIVCPICSQKP
Q8QRD3  MHGDTPTLHEYMLDLQPETTDLYCYEQLNDSSEEEDEINGPAGQAEPDRAHYNIVTFCCKCDSTLRLCVQSTHVDIRTLEDLLMGTLGIVCPICSQKP
Q8QRD4  MHGDTPTLHEYMLDLQPETTDLYCYEQLSDSSEEEDEIDGPAGQAEPDRAHYNIVTFCCKCDSTLWLCVQSTHVDIRTLEDLLMGTLGIVCPICSQKP
Q8V1J0  MHGDTPTLHEYMLDLQPETTDLYCYEQLNDSSEEEDEIDGPAGQAEPDRAHYNIVTFCCKCDSTLRLCVQSTHVDICTLEDLLMGTLGIVCPICSRKP
P03129  MHGDTPTLHEYMLDLQPETTDLYCYEQLNDSSEEEDEIDGPAGQAEPDRAHYNIVTFCCKCDSTLRLCVQSTHVDIRTLEDLLMGTLGIVCPICSQKP
        **************:****:*******: * *******:******:**************** **  ********* :*****************:**
```

FIGURE 10. **Conservation of $E7_{11-19}$ in all high risk HPV-16 strains.** 15 of the 16 HPV-16 E7 sequences in the HPV data base include the $E7_{11-19}$ sequence. The corresponding UniProt accession number of each sequence is shown at the *left of each line*. *Asterisk*, this column contains identical amino acid residues in all sequences; *colon*, this column contains different but highly conserved (very similar) amino acids; no symbol indicates that this column contains dissimilar amino acids or gaps.

A

A0201	10.88	A0221	10.77	A0243	10.88	A0264	115.46	A0285	10.88	A9209	10.88
A0202	24.63	A0222	56.17	A0244	10.23	A0265	6749.70	A0286	10.88	A9210	473.5
A0203	34.53	A0224	10.88	A0245	34.63	A0266	10.88	A0287	66.36	A9211	10.88
A0204	65.76	A0225	10.88	A0246	14.96	A0267	10.88	A0289	10.88	A9212	3012.35
A0205	70.01	A0226	10.16	A0247	26.17	A0268	10.88	A0290	10.52	A9214	643.44
A0206	10.77	A0227	10.11	A0248	11.55	A0269	3.07	A0291	10.77	A9215	24.63
A0207	1788.06	A0228	10.77	A0249	14.50	A0270	10.88	A0292	14.96	A9216	12.07
A0208	570.53	A0229	16.96	A0250	168.87	A0271	10.88	A0293	10.88	A9217	2262.26
A0209	10.88	A0230	10.88	A0251	10.77	A0272	10.77	A0295	10.88	A9218	10.88
A0210	140.65	A0231	10.88	A0252	81.98	A0273	33.23	A0296	10.88	A9219	10.88
A0211	3.07	A0233	59.93	A0254	36.02	A0274	10.88	A0297	10.88	A9220	10.88
A0212	12.91	A0234	86.42	A0255	2005.08	A0275	10.88	A0299	7.89	A9221	10.88
A0213	10.67	A0235	72.62	A0256	2582.10	A0276	7.66	A9201	26.97	A9222	507.87
A0214	8.65	A0236	26.88	A0257	77.24	A0277	10.88	A9202	24.63	A9223	10.88
A0215	1788.06	A0237	33.59	A0258	6.80	A0278	1489	A9203	29825.20	A9224	39.37
A0216	6.07	A0238	20.99	A0259	10.88	A0279	10.77	A9204	56.17	A9226	10.77
A0217	473.5	A0239	79.32	A0260	20.36	A0280	687.20	A9205	21.07		
A0218	1788.06	A0240	10.88	A0261	10.77	A0281	39.37	A9206	10.77		
A0219	33.59	A0241	20.02	A0262	724.08	A0283	10.88	A9207	10.88		
A0220	77.96	A0242	16.88	A0263	24.63	A0284	6.43	A9208	974.66		

Strong
Weak

B

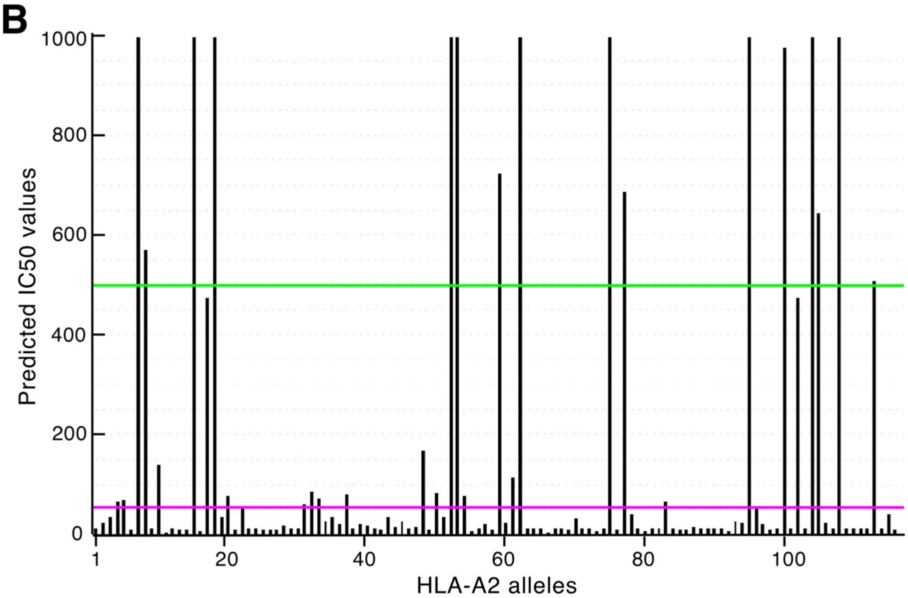

FIGURE 11. **$E7_{11-19}$ binds to the vast majority of HLA-A2 alleles.** HLA binding predictions of $E7_{11-19}$ were performed using NetMHCpan on the 116 known HLA-A2 alleles. *Panel A* shows the predicted IC_{50} values for each allele (in nM) with strong binding (<50 nM) *shaded magenta*, weak binding (50–500 nM) *shaded green*, and no binding (>500 nM) unshaded. *Panel B* gives a *bar graph* representation of $E7_{11-19}$ IC_{50} for each allele along the *x* axis corresponding to those going from the *left* to *right columns* in the order defined in *panel A*.

two transfectant cell lines, N/E6E7 and OKF6/E6E7, have comparable amounts to the episomal cell line.

The striking specificity of human CTL for $E7_{11-19}$ is worth underscoring. $E7_{11-19}$-specific T cells recognize and lysed $E7_{11-19}$-loaded but not $E7_{11-20}$-loaded target cells even though both peptides bind well to HLA-A*0201. Alloreactivity as a basis for cytotoxicity in the assay was excluded by using a peptide pulsed autologous B cell line (Laz 509) as a target. Although not shown, $E7_{11-20}$ 10-mer-specific T cells lysed autologous $E7_{11-20}$ but not $E7_{11-19}$-pulsed B cells as well. Why should this recognition be so discrete in view of the fact that the two peptides differ from one another by only a single carboxyl-terminal threonine residue? The answer lies in the general nature of peptide binding to MHC class I molecules. One pocket exists for the amino terminus and a second for the carboxylate of the peptide, thereby docking the peptide ends in the HLA groove between $\alpha 1$ and $\alpha 2$ helices. The fixed "ends" mandate that the 10-mer peptide bulges further out of the HLA binding groove than the 9-mer, with greater surface area exposed to the TCR. Both the position of the main chain and side chain positions are altered. Hence, these two peptides will differ in their TCR recognition features (Ref. 76 and references therein). Failure to identify the precise epitope for use in the vaccine elicitation strategy will likely engender a misdirected response even for such similar sequences.

A recent study of 19 women with grade 3 vulvar intraepithelial neoplasia vaccinated with a non-epitope targeted mix of long peptides from HPV-16 viral E6 and E7 oncoproteins in incomplete Freund's adjuvant showed promising clinical responses (35). At 3 months post-vaccination, 5 women had complete regression, and at 12 months, 79% of subjects appeared to show significant clinical responses. These results demonstrate that therapeutic vaccination harnessing cellular immunity can be effective. But vaccinating with any set of long peptides that span the target antigen and incorporate the expected T cell epitopes is unlikely to be optimal. Broad and nonselective immune responses arising from an uncharacterized processing of vaccine components in secondary lymphoid organs coupled with restricted presentation by primary tumor cells would limit the population of responding CTLs at the tumor and therein directly reduce TCR-mediated cytolysis and secondarily dilute requisite inflammatory signals in the microenvironment. Dendritic cell presentation of multiple T cell epitopes, few of which are relevant, combined with well known mechanisms of immunodominance may further result in misguided responses (76). Targeting a response in a precise way in future immunotherapeutic efforts offering appropriate adjuvant and delivery to dendritic cells will focus T cells on relevant protective/therapeutic epitopes. In addition, by precisely selecting T cell epitopes in vaccine formulation, bioinformatics can be used to calculate population protection coverage, ensuring that there is an adequate breadth of epitopes incorporated.

The landmark studies of Benacerraf (77) on immune response genes demonstrated many years ago that immune responses to chemically defined antigens are strictly dependent on MHC alleles. In this regard, the basis for the complete response in only a subset of patients with vulvar intraepithelial neoplasia (35) is almost certainly related to differences in HLA alleles expressed by the subjects. An analysis of the frequencies of HLA-A, -B, and -C alleles in the five major ethnic groups of the United States involving 1296 unrelated subjects from five major outbred groups (African American, Caucasians, Asian, Hispanic, and North American Natives) was performed (78). The frequency of A*0201, which binds strongly to $E7_{11-19}$, is higher than 10% in each group aside from Asians. In the Korean population, A*0201 and A*0206, which are $E7_{11-19}$ binding alleles, compose 85% of the A2 positive population (79). Among the 16 HLA-A2 alleles that are not predicted to bind $E7_{11-19}$, we find that A*0207, A*0278, A*9208 and A*9217 are found in the Chinese population, with the frequency of A*0207 higher than 10% in the southern Chinese Han population (80, 81).

Nine major HLA class I supertypes (A1, A2, A3, A24, B7, B27, B44, B58, and B62) have been identified (82). Each of the four HLA class I supertypes (A2, A3, B7, and B44) allows coverage of about 35–55% of the general population regardless of ethnicity (83). When epitopes from the A2, A3, B7, and B44 supertypes are combined, general population coverage is higher than 90%. Common alleles of the four supertypes are: A2 (A*0201-07, A*6802, and A*6901), A3 (A*0301, A*1101, A*3101, A*3301, and A*6801), B7 (B*0702, B*3501–03, B*5101-02, B*5301, and B*5401) and B4 (B*3701, B*4001, B*4006, B*4402, and B*4403). Within the A2 supertype, predicted binding affinities for the conserved $E7_{11-19}$ epitope to A*0201, A*0202, A*0203, A*0204, A*0205, and A*0206 are excellent (Fig. 11). By selecting for promiscuous peptide binders parsed for conservation of sequence among viruses and whose presentation on target cells is verified by physical methods, a new paradigm for T cell-based vaccines can evolve predicated on T cell epitope specificity and precise HLA restriction. This paradigm should be added to vaccinology in the genomic era (84).

Our results strongly imply that the presence or absence of memory responses in the peripheral blood is not a useful surrogate to guide immunity to relevant tumor target antigens. Precursor frequencies may be too low, especially if cells have already trafficked to target organs as effector memory populations. Moreover, as antigen is transported to lymph node and presented to T cells on dendritic cells, a focusing of immune response through cross-presentation or other means may select for immunodominant epitopes not necessarily reflective of relevant peptide array displayed on tumor cells. Immune responses against the latter are what will lead to protection. The MS technology described here offers an approach toward making identification of such a display tractable using a limited number of cells.

Acknowledgments—We thank K. Münger (Channing Laboratory, Department of Medicine, Brigham and Women's Hospital/Harvard Medical School) for expert advice and review of this manuscript and J. H. Lee (Department of Otolaryngology, University of Iowa) and James G. Rheinwald (Department of Dermatology and Harvard Skin Disease Research Center, Brigham and Women's Hospital and Harvard Medical School) for kind gifts of the C66 and E6E7 cell lines, respectively.

REFERENCES

1. zur Hausen, H. (1977) *Curr. Top. Microbiol. Immunol.* **78,** 1–30
2. Kreimer, A. R., Clifford, G. M., Boyle, P., and Franceschi, S. (2005) *Cancer Epidemiol. Biomarkers Prev.* **14,** 467–475
3. Munoz, N., Castellsague, X., de Gonzalez, A. B., and Gissmann, L. (2006) *Vaccine* **24,** Suppl. 3, 1–10
4. Moscicki, A. B., Schiffman, M., Kjaer, S., and Villa, L. L. (2006) *Vaccine* **24,** Suppl S3, 42–51
5. Longworth, M. S., and Laimins, L. A. (2004) *Microbiol. Mol. Biol. Rev.* **68,** 362–372
6. Münger, K., Baldwin, A., Edwards, K. M., Hayakawa, H., Nguyen, C. L., Owens, M., Grace, M., and Huh, K. (2004) *J. Virol.* **78,** 11451–11460
7. Parkin, D. M., and Bray, F. (2006) *Vaccine* **24,** Suppl 3, S3/11–25
8. Berzofsky, J. A., Ahlers, J. D., Janik, J., Morris, J., Oh, S., Terabe, M., and Belyakov, I. M. (2004) *J. Clin. Invest.* **114,** 450–462
9. Lowy, D. R., and Schiller, J. T. (2006) *J. Clin. Invest.* **116,** 1167–1173
10. Printz, C. (2009) *Cancer* **115,** 5130
11. Ramqvist, T., Andreasson, K., and Dalianis, T. (2007) *Expert Opin. Biol. Ther.* **7,** 997–1007
12. Vetter, K. M., and Geller, S. E. (2007) *J. Womens Health* **16,** 1258–1268
13. Frazer, I. H. (2004) *Nat. Rev. Immunol* **4,** 46–54
14. Stanley, M. (2006) *Vaccine* **24,** Suppl 1S, 16–22
15. Boon, T., Coulie, P. G., and Van den Eynde, B. (1997) *Immunol Today* **18,** 267–268
16. Devaraj, K., Gillison, M. L., and Wu, T. C. (2003) *Crit. Rev. Oral. Biol. Med.* **14,** 345–362
17. Leggatt, G. R., and Frazer, I. H. (2007) *Curr. Opin. Immunol.* **19,** 232–238

18. Roden, R. B., Ling, M., and Wu, T. C. (2004) *Hum. Pathol.* **35,** 971–982
19. Peng, S., Trimble, C., Wu, L., Pardoll, D., Roden, R., Hung, C. F., and Wu, T. C. (2007) *Clin. Cancer Res.* **13,** 2479–2487
20. García-Hernández, E., González-Sánchez, J. L., Andrade-Manzano, A., Contreras, M. L., Padilla, S., Guzmán, C. C., Jiménez, R., Reyes, L., Morosoli, G., Verde, M. L., and Rosales, R. (2006) *Cancer Gene Ther.* **13,** 592–597
21. Albarran, Y., Carvajal, A., de la Garza, A., Cruz Quiroz, B. J., Vazquez Zea, E., Díaz Estrada, I., Mendez Fuentez, E., López Contreras, M., Andrade-Manzano, A., Padilla, S., Varela, A. R., and Rosales, R. (2007) *BioDrugs* **21,** 47–59
22. Kaufmann, A. M., Stern, P. L., Rankin, E. M., Sommer, H., Nuessler, V., Schneider, A., Adams, M., Onon, T. S., Bauknecht, T., Wagner, U., Kroon, K., Hickling, J., Boswell, C. M., Stacey, S. N., Kitchener, H. C., Gillard, J., Wanders, J., Roberts, J. S., and Zwierzina, H. (2002) *Clin. Cancer Res.* **8,** 3676–3685
23. Einstein, M. H., Kadish, A. S., Burk, R. D., Kim, M. Y., Wadler, S., Streicher, H., Goldberg, G. L., and Runowicz, C. D. (2007) *Gynecol. Oncol.* **106,** 453–460
24. Palefsky, J. M., Berry, J. M., Jay, N., Krogstad, M., Da Costa, M., Darragh, T. M., and Lee, J. Y. (2006) *Aids* **20,** 1151–1155
25. Derkay, C. S., Smith, R. J., McClay, J., van Burik, J. A., Wiatrak, B. J., Arnold, J., Berger, B., and Neefe, J. R. (2005) *Ann. Otol. Rhinol. Laryngol.* **114,** 730–737
26. Fiander, A. N., Tristram, A. J., Davidson, E. J., Tomlinson, A. E., Man, S., Baldwin, P. J., Sterling, J. C., and Kitchener, H. C. (2006) *Int. J. Gynecol Cancer* **16,** 1075–1081
27. Hallez, S., Simon, P., Maudoux, F., Doyen, J., Noël, J. C., Beliard, A., Capelle, X., Buxant, F., Fayt, I., Lagrost, A. C., Hubert, P., Gerday, C., Burny, A., Boniver, J., Foidart, J. M., Delvenne, P., and Jacobs, N. (2004) *Cancer Immunol. Immunother.* **53,** 642–650
28. Kast, W. M., Brandt, R. M., Drijfhout, J. W., and Melief, C. J. (1993) *J. Immunother. Emphasis Tumor Immunol.* **14,** 115–120
29. Feltkamp, M. C., Smits, H. L., Vierboom, M. P., Minnaar, R. P., de Jongh, B. M., Drijfhout, J. W., ter Schegget, J., Melief, C. J., and Kast, W. M. (1993) *Eur. J. Immunol.* **23,** 2242–2249
30. Ressing, M. E., Sette, A., Brandt, R. M., Ruppert, J., Wentworth, P. A., Hartman, M., Oseroff, C., Grey, H. M., Melief, C. J., and Kast, W. M. (1995) *J. Immunol.* **154,** 5934–5943
31. Steller, M. A., Gurski, K. J., Murakami, M., Daniel, R. W., Shah, K. V., Celis, E., Sette, A., Trimble, E. L., Park, R. C., and Marincola, F. M. (1998) *Clin. Cancer Res.* **4,** 2103–2109
32. van Driel, W. J., Ressing, M. E., Kenter, G. G., Brandt, R. M., Krul, E. J., van Rossum, A. B., Schuuring, E., Offringa, R., Bauknecht, T., Tamm-Hermelink, A., van Dam, P. A., Fleuren, G. J., Kast, W. M., Melief, C. J., and Trimbos, J. B. (1999) *Eur. J. Cancer* **35,** 946–952
33. Ressing, M. E., van Driel, W. J., Brandt, R. M., Kenter, G. G., de Jong, J. H., Bauknecht, T., Fleuren, G. J., Hoogerhout, P., Offringa, R., Sette, A., Celis, E., Grey, H., Trimbos, B. J., Kast, W. M., and Melief, C. J. (2000) *J. Immunother.* **23,** 255–266
34. Muderspach, L., Wilczynski, S., Roman, L., Bade, L., Felix, J., Small, L. A., Kast, W. M., Fascio, G., Marty, V., and Weber, J. (2000) *Clin. Cancer Res.* **6,** 3406–3416
35. Kenter, G. G., Welters, M. J., Valentijn, A. R., Lowik, M. J., Berends-van der Meer, D. M., Vloon, A. P., Essahsah, F., Fathers, L. M., Offringa, R., Drijfhout, J. W., Wafelman, A. R., Oostendorp, J., Fleuren, G. J., van der Burg, S. H., and Melief, C. J. (2009) *N. Engl. J. Med.* **361,** 1838–1847
36. Rudolph, M. G., Stanfield, R. L., and Wilson, I. A. (2006) *Annu. Rev. Immunol.* **24,** 419–466
37. Wang, J. H., and Reinherz, E. L. (2002) *Mol. Immunol.* **38,** 1039–1049
38. Robinson, J., Waller, M. J., Fail, S. C., McWilliam, H., Lopez, R., Parham, P., and Marsh, S. G. (2009) *Nucleic Acids Res.* **37,** D1013–D1017
39. Brusic, V., August, J. T., and Petrovsky, N. (2005) *Expert Rev. Vaccines* **4,** 407–417
40. De Groot, A. S., and Berzofsky, J. A. (2004) *Methods* **34,** 425–428
41. Purcell, A. W., McCluskey, J., and Rossjohn, J. (2007) *Nat. Rev. Drug Discov.* **6,** 404–414
42. Lee, J. H., Yi, S. M., Anderson, M. E., Berger, K. L., Welsh, M. J., Klingelhutz, A. J., and Ozbun, M. A. (2004) *Proc. Natl. Acad. Sci. U.S.A.* **101,** 2094–2099
43. Lin, H. H., Ray, S., Tongchusak, S., Reinherz, E. L., and Brusic, V. (2008) *BMC Immunol.* **9,** 8
44. Zhong, W., Reche, P. A., Lai, C. C., Reinhold, B., and Reinherz, E. L. (2003) *J. Biol. Chem.* **278,** 45135–45144
45. Schultze, J. L., Michalak, S., Seamon, M. J., Dranoff, G., Jung, K., Daley, J., Delgado, J. C., Gribben, J. G., and Nadler, L. M. (1997) *J. Clin. Invest.* **100,** 2757–2765
46. Kast, W. M., Brandt, R. M., Sidney, J., Drijfhout, J. W., Kubo, R. T., Grey, H. M., Melief, C. J., and Sette, A. (1994) *J. Immunol.* **152,** 3904–3912
47. Arnold, D., Driscoll, J., Androlewicz, M., Hughes, E., Cresswell, P., and Spies, T. (1992) *Nature* **360,** 171–174
48. Momburg, F., Ortiz-Navarrete, V., Neefjes, J., Goulmy, E., van de Wal, Y., Spits, H., Powis, S. J., Butcher, G. W., Howard, J. C., Walden, P., and Hammerling, G. (1992) *Nature* **360,** 174–177
49. Muñoz, N., Bosch, F. X., Castellsagué, X., Díaz, M., de Sanjose, S., Hammouda, D., Shah, K. V., and Meijer, C. J. (2004) *Int. J. Cancer* **111,** 278–285
50. van den Hende, M., van Poelgeest, M. I., van der Hulst, J. M., de Jong, J., Drijfhout, J. W., Fleuren, G. J., Valentijn, A. R., Wafelman, A. R., Slappendel, G. M., Melief, C. J., Offringa, R., van der Burg, S. H., and Kenter, G. G. (2008) *Int. J. Cancer* **123,** 146–152
51. Henderson, R. A., Michel, H., Sakaguchi, K., Shabanowitz, J., Appella, E., Hunt, D. F., and Engelhard, V. H. (1992) *Science* **255,** 1264–1266
52. Cento, V., Ciccozzi, M., Ronga, L., Perno, C. F., and Ciotti, M. (2009) *J. Med. Virol.* **81,** 1627–1634
53. Hoof, I., Peters, B., Sidney, J., Pedersen, L. E., Sette, A., Lund, O., Buus, S., and Nielsen, M. (2009) *Immunogenetics* **61,** 1–13
54. Schiller, J. T., Castellsague, X., Villa, L. L., and Hildesheim, A. (2008) *Vaccine* **26,** Suppl 10, K53–61
55. Kadish, A. S., Ho, G. Y., Burk, R. D., Wang, Y., Romney, S. L., Ledwidge, R., and Angeletti, R. H. (1997) *J. Natl. Cancer Inst.* **89,** 1285–1293
56. Bourgault Villada, I., Bénéton, N., Bony, C., Connan, F., Monsonego, J., Bianchi, A., Saiag, P., Lévy, J. P., Guillet, J. G., and Choppin, J. (2000) *Eur. J. Immunol.* **30,** 2281–2289
57. van der Burg, S. H., Ressing, M. E., Kwappenberg, K. M., de Jong, A., Straathof, K., de Jong, J., Geluk, A., van Meijgaarden, K. E., Franken, K. L., Ottenhoff, T. H., Fleuren, G. J., Kenter, G., Melief, C. J., and Offringa, R. (2001) *Int. J. Cancer* **91,** 612–618
58. Rudolf, M. P., Man, S., Melief, C. J., Sette, A., and Kast, W. M. (2001) *Clin. Cancer Res.* **7,** 788s–795s
59. Kather, A., Ferrara, A., Nonn, M., Schinz, M., Nieland, J., Schneider, A., Dürst, M., and Kaufmann, A. M. (2003) *Int. J. Cancer* **104,** 345–353
60. Bourgault Villada, I., Moyal Barracco, M., Villada, I. B., Barracco, M. M., Ziol, M., Chaboissier, A., Barget, N., Berville, S., Paniel, B., Jullian, E., Clerici, T., Maillère, B., and Guillet, J. G. (2004) *Cancer Res.* **64,** 8761–8766
61. Nakagawa, M., Kim, K. H., and Moscicki, A. B. (2004) *Clin. Diagn. Lab. Immunol.* **11,** 889–896
62. Warrino, D. E., Olson, W. C., Knapp, W. T., Scarrow, M. I., D'Ambrosio-Brennan, L. J., Guido, R. S., Edwards, R. P., Kast, W. M., and Storkus, W. J. (2004) *Clin. Cancer Res.* **10,** 3301–3308
63. Sarkar, A. K., Tortolero-Luna, G., Follen, M., and Sastry, K. J. (2005) *Gynecol. Oncol.* **99,** S251–S261
64. Hara, M., Matsueda, S., Tamura, M., Takedatsu, H., Tanaka, M., Kawano, K., Mochizuki, K., Kamura, T., Itoh, K., and Harada, M. (2005) *Int. J. Oncol.* **27,** 1371–1379
65. Oerke, S., Höhn, H., Zehbe, I., Pilch, H., Schicketanz, K. H., Hitzler, W. E., Neukirch, C., Freitag, K., and Maeurer, M. J. (2005) *Int. J. Cancer* **114,** 766–778
66. Nakagawa, M., Kim, K. H., Gillam, T. M., and Moscicki, A. B. (2007) *J. Virol.* **81,** 1412–1423
67. Gallagher, K. M., and Man, S. (2007) *J. Gen Virol.* **88,** 1470–1478
68. Morishima, S., Akatsuka, Y., Nawa, A., Kondo, E., Kiyono, T., Torikai, H., Nakanishi, T., Ito, Y., Tsujimura, K., Iwata, K., Ito, K., Kodera, Y., Morishima, Y., Kuzushima, K., and Takahashi, T. (2007) *Int. J. Cancer* **120,** 594–604
69. Piersma, S. J., Welters, M. J., van der Hulst, J. M., Kloth, J. N., Kwappenberg, K. M., Trimbos, B. J., Melief, C. J., Hellebrekers, B. W., Fleuren, G. J.,

Kenter, G. G., Offringa, R., and van der Burg, S. H. (2008) *Int. J. Cancer* **122,** 486–494
70. Tindle, R. W. (2002) *Nat. Rev. Cancer* **2,** 59–65
71. Kanodia, S., Fahey, L. M., and Kast, W. M. (2007) *Curr. Cancer Drug Targets* **7,** 79–89
72. Stanley, M. A., Pett, M. R., and Coleman, N. (2007) *Biochem. Soc. Trans.* **35,** 1456–1460
73. Georgopoulos, N. T., Proffitt, J. L., and Blair, G. E. (2000) *Oncogene* **19,** 4930–4935
74. Brady, C. S., Bartholomew, J. S., Burt, D. J., Duggan-Keen, M. F., Glenville, S., Telford, N., Little, A. M., Davidson, J. A., Jimenez, P., Ruiz-Cabello, F., Garrido, F., and Stern, P. L. (2000) *Tissue Antigens* **55,** 401–411
75. Steger, G., and Corbach, S. (1997) *J. Virol.* **71,** 50–58
76. Meijers, R., Lai, C. C., Yang, Y., Liu, J. H., Zhong, W., Wang, J. H., and Reinherz, E. L. (2005) *J. Mol. Biol.* **345,** 1099–1110
77. Benacerraf, B. (1980) *Nobel Lecture Physiology or Medicine 1971–1980* (1992) (Lindsten, J., ed) pp. 597–623, World Scientific Publishing Co., Singapore
78. Cao, K., Hollenbach, J., Shi, X., Shi, W., Chopek, M., and Fernández-Viña, M. A. (2001) *Hum. Immunol.* **62,** 1009–1030
79. Lee, K. W., Oh, D. H., Lee, C., and Yang, S. Y. (2005) *Tissue Antigens* **65,** 437–447
80. Gao, S. Q., Zou, H. Y., Cheng, L. H., Jing, S. Z., and Deng, Z. H. (2009) *Zhonghua Yi Xue Yi Chuan Xue Za Zhi* **26,** 228–232
81. Yao, Y., Shi, L., Shi, L., Matsushita, M., Yu, L., Lin, K., Tao, Y., Huang, X., Yi, W., Oka, T., Tokunaga, K., and Chu, J. (2009) *Tissue Antigens* **73,** 561–568
82. Sette, A., and Sidney, J. (1999) *Immunogenetics* **50,** 201–212
83. Sidney, J., Grey, H. M., Kubo, R. T., and Sette, A. (1996) *Immunol Today* **17,** 261–266
84. Rinaudo, C. D., Telford, J. L., Rappuoli, R., and Seib, K. L. (2009) *J. Clin. Invest.* **119,** 2515–2525
85. Ashrafi, G. H., Haghshenas, M., Marchetti, B., and Campo, M. S. (2006) *Int. J. Cancer* **119,** 2105–2112
86. Davy, C. E., Ayub, M., Jackson, D. J., Das, P., McIntosh, P., and Doorbar, J. (2006) *Virology* **349,** 230–244
87. Davy, C. E., Jackson, D. J., Raj, K., Peh, W. L., Southern, S. A., Das, P., Sorathia, R., Laskey, P., Middleton, K., Nakahara, T., Wang, Q., Masterson, P. J., Lambert, P. F., Cuthill, S., Millar, J. B., and Doorbar, J. (2005) *J. Virol.* **79,** 3998–4011
88. Dyson, N., Howley, P. M., Münger, K., and Harlow, E. (1989) *Science* **243,** 934–937
89. Kabsch, K., and Alonso, A. (2002) *J. Virol.* **76,** 12162–12172
90. McIntosh, P. B., Martin, S. R., Jackson, D. J., Khan, J., Isaacson, E. R., Calder, L., Raj, K., Griffin, H. M., Wang, Q., Laskey, P., Eccleston, J. F., and Doorbar, J. (2008) *J. Virol.* **82,** 8196–8203
91. O'Brien, P. M., and Saveria Campo, M. (2002) *Virus Res.* **88,** 103–117
92. Werness, B. A., Levine, A. J., and Howley, P. M. (1990) *Science* **248,** 76–79
93. Zhang, B., Li, P., Wang, E., Brahmi, Z., Dunn, K. W., Blum, J. S., and Roman, A. (2003) *Virology* **310,** 100–108
94. Pattillo, R. A., Hussa, R. O., Story, M. T., Ruckert, A. C., Shalaby, M. R., and Mattingly, R. F. (1977) *Science* **196,** 1456–1458